TOWARDS VIABLE METHODS TO COMPUTE NONLINEAR OPTICAL PROPERTIES FOR BIOCHEMICAL SYSTEMS

TOWARDS VIABLE METHODS TO COMPUTE NONLINEAR OPTICAL PROPERTIES FOR BIOCHEMICAL SYSTEMS

By

ANAND PATEL

Hon. B.Sc. (Chemical Biology)

A Thesis

Submitted to the School of Graduate Studies

In Partial Fulfillment of the Requirements for the Degree

Master of Science

McMaster University

(Chemistry & Chemical Biology) Hamilton, Ontario, Canada

TITLE: Towards Viable Methods to Compute Nonlinear Optical Properties for Biochemical Systems

AUTHOR: Anand Patel (B.Sc. Chemical Biology, McMaster University)

SUPERVISOR: Professor Paul W. Ayers

NUMBER OF PAGES: x, 76

ABSTRACT

Though quantum chemical tools are routinely used for computing the properties of chemical systems, barriers still remain for the widespread use of these tools in a more biological context. In particular, the computation of nonlinear optical properties remains a difficult calculation, despite the usefulness of these phenomena to bioimaging, pharmaceutical development, and microscopy. This thesis aims to produce new methods that would help make the computation of nonlinear optical properties easier for molecules and systems important for biological contexts. We propose to do this in two parts: (1) to improve the existing finite field method for NLO property prediction through use of a rational function fitting model, and (2) to use resummation as a computationally cheap means of refining the accuracy of relatively cheap energy calculation methods. Overall, this work found that the rational model does produce a more robust finite field method when compared to the traditional polynomial-based finite field method. Though the resummation method shows early promise, it still tends to have issues with optimization and particular systems that need to be overcome.

ACKNOWLEGEMENTS

I would like to first express my deepest gratitude to my supervisor, Dr. Paul Ayers. He is someone who has consistently gone above and beyond the call of duty as a mentor. Not only is he someone who provides amazing scientific guidance and insight, but he is also one of the kindest, and most caring people that I've had the fortune of working for. Without Paul's guidance and support, I would not be where I am today.

I would also like to express my heartfelt thanks to Farnaz Heidar-Zadeh, who supervised me throughout my summer research terms, and the duration of my undergraduate thesis.

I would like to thank all the members of the Ayers Group. It seems that the several years working in the Ayers Group have flown by, not in the least due to the wonderful people that I had the opportunity to call colleagues, and more often than not, friends.

I would like to thank my parents, Nita and Harshad Patel, who have been putting up with me asking "why?" ever since I learned the word. Thank you for always encouraging me to dream big!

Table of Contents

List of Figures

List of Tables

Preface

This thesis contains both published and unpublished content. This chapter details my contributions to each chapter. The coauthors of any published works can also be found in the footnotes of the corresponding chapter.

This thesis consists of four chapters, including an introduction and summary. The introduction serves as an outline to the second and third chapters, along with providing insight into the motivation for this work, and a general overview of the field as a whole. The introduction also provides background into potential future work that may be undertaken to build on the results of this thesis. Chapter 2 is a published journal article, while Chapter 3 is an unpublished piece of work. The summary contains details of the works performed, along with an analysis of directions that future work may take.

Chapter 2 is a reprint of the "Finite Field Method for Nonlinear Optical Property Prediction Using Rational Function Approximants" article, published in the *Journal of Physical Chemistry A*. I am the first author on this paper, while Ahmed A.K. Mohammed, Peter A. Limacher, and Paul W. Ayers are the second, third and fourth co-authors on this paper, respectively. I programmed the calculations for the rational function model calculations, and ran the corresponding calculations. I also wrote the first draft of the manuscript, with input and editing from Ahmed Mohammed, Peter Limacher and Paul Ayers. The latter three authors also performed the final edits to the paper.

Chapter 3 is unpublished work that was performed in conjunction with Nadin Abbas , Cristina E. González-Espinoza, and Paul W. Ayers. My role in the work was to write the program to implement the method, along with running some of the electronic

structure calculations. I also supervised Nadin Abbas on this project, who also ran electronic structure calculations, and ran the code to get results from the method, with some guidance from me. Cristina González-Espinoza wrote code for the future directions of this project, along with providing valuable programming guidance. Paul Ayers provided the overall structure of the project, and the ideas; he also provided valuable guidance throughout the project.

Chapter 1

Introduction

1.1 Motivation

With the discovery of nonlinear optical phenomena in 1961[1], there has been an ever-increasing interest in understanding and characterizing these properties. This is largely due to the importance of these phenomena in fields such as organic chemistry, materials science, and spectroscopy, among others.[2] These phenomena are also highly relevant to potential technologies that may be useful into the future, such as the creation of optical processors, which use light rather than transistors to relay information.[3]

With the relevance to many highly exciting fields, the interest in computing these properties has only grown.[3,4] Computing nonlinear optical (NLO) properties offers

several advantages to the experimental approach, including faster and cheaper characterization of a material's properties. This would potentially allow for a more rational design of materials with desired NLO properties and also for computational prescreening of prospective NLO materials, allowing the time-consuming and sometimes expensive processes of experimental synthesis and characterization to be limited to the most promising substances.

Despite the advantages that are offered by computational tools, there are several drawbacks. The available tools will be discussed in more detail in further sections, but most relevantly, most tools lack the ability to quickly and accurately determine the properties of large and complex systems, including the macromolecules of biological relevance. This is often due to the size of these systems, which are generally much larger than those typically treated by most computational chemistry tools. For example, though NLO properties may be exploited to provide high-contrast confocal imaging of biological samples[5], only particular dyes may be used for this purpose[6]. One use of a tool able to look at NLO properties for larger systems may be the creation of novel imaging dyes for confocal microscopy. There are a myriad of other uses that may be fathomed for a tool of this nature, which will be further discussed in a later section.

The dilemma presented by looking at larger systems is the classic one of scale. Using quantum chemistry tools for large-scale problems is akin to cutting a lawn with scissors. There are two major limitations that prohibit the use of most quantum chemical tools, which are the computation of energies for large systems, and determining a reliable, robust and quick method for the computation of the actual NLO properties themselves. This thesis aims to address both these problems in subsequent chapters,

through the mathematical lens of function fitting, in order to solve problems that are relevant to the fields of biochemistry and chemical biology.

1.2 Background of Nonlinear Optics

1.2.1 Overview

For most materials, light does not alter the optical properties of the material itself.[2] This means that the polarization induced in the material is linearly related to the strength of the electric field in the light, through the following equation:

$$\mu = \alpha F \qquad \text{Eq. 1.2.1}$$

Where μ is the dipole moment of the molecule, and α is the polarizability of the molecule in response to an electric field *F*. However, under particular conditions, usually the application of intense light to an appropriate material, one can observe nonlinear optical effects. These nonlinear effects were first observed in 196[1]1 and, since then, interest in the field has grown dramatically. Nonlinear optics describes the branch of optical phenomena that arise when materials have a nonlinear response to light.[2] Mathematically, this is when the polarization induced in the material by the light, and the electric field of the light is related through the following equation:

$$E(F) = E(0) + \left.\frac{\partial E}{\partial F}\right|_0 F + \frac{1}{2!}\left.\frac{\partial^2 E}{\partial F^2}\right|_0 F^2 + \frac{1}{3!}\left.\frac{\partial^3 E}{\partial F^3}\right|_0 F^3 + \frac{1}{4!}\left.\frac{\partial^4 E}{\partial F^4}\right|_0 F^4 + \cdots \qquad \text{Eq. 1.2.2}$$

Where *F* is the electric field strength, and *E* is the energy of the molecule. We can make the following substitutions into the equation:

$$E(F) = E(0) - \mu F - \frac{1}{2}\alpha F^2 - \frac{1}{6}\beta F^3 - \frac{1}{24}\gamma F^4 + \cdots \qquad \text{Eq. 1.2.3}$$

The terms α, β, and γ are the polarizability, hyperpolarizability, and second hyperpolarizability, respectively. These terms are considered to be the nonlinear optical properties of interest to many fields.

In general, each of these properties holds significance with regards to observed natural phenomena.[2,7] For example, the α coefficient is related to the refractive index of the material. One major phenomena that arises from the coefficient β is harmonic generation, where two or more photons with a particular frequency are destroyed, to produce a photon with a higher frequency than those of the original photons. This would be of particular importance to spectroscopists, who rely on exploiting these phenomena to produce more contrast while imaging. The third hyperpolarizability, γ, is related to third harmonic generation, similar to second harmonic generation, but with three photons being destroyed to produce a single photon of a higher frequency. Additionally γ is related to other processes, such as simulated Raman scattering, and may be relevant to the fields of optical computing and switching.

1.2.2 Experimental Approaches to Determine NLO Properties

The experimental approach to determining NLO properties is perhaps the most direct one. However, this approach has both advantages and disadvantages. The largest advantage to performing experimental measurements is the confidence in one's results, provided that the measurements were done appropriately. The drawbacks to this approach are the time involved with running experiments, the cost to buy the appropriate materials and equipment, and the expertise required for the measurements to be accurate.

To perform experimental measurements of NLO properties, there are several generally accepted methods. For the polarizability, α, one can measure the relative dielectric permittivity[8] or determine the refractive index[9]. To determine the hyperpolarizability, β, one can use hyper-Rayleigh scattering[10,11], or electric-field induced second harmonic generation[12]. In general, the former is preferred because it is a simpler experimental procedure than the latter. For the second hyperpolarizability, γ, one can use harmonic generation[12] or four-wave mixing[13]. No viable experimental methods of measuring higher order hyperpolarizabilities, such as δ, are available. However, these higher order hyperpolarizabilities may be determined via computational methods.

1.2.3 Computing NLO Properties

Computational tools to investigate NLO properties present an attractive alternative to the experimental approach, as these tools can often screen for properties in a fraction of the time that it would take for experimental characterization. There are many computational tools available, each of which relies on different approaches. The approach to take highly depends on the accuracy desired, the computational power available, and the timeframe in which the computations must be completed.

There are currently numerous options available to compute nonlinear optical properties. These methods include sum-over-states, coupled-perturbed Hartree-Fock, response theory, and the finite field method. Each of these methods have strengths and weaknesses.

The sum-over-states[14–16] approach is grounded in the Configuration Interaction with single excitations (CIS), though it can be generalized to more elaborate

configuration-interaction wavefunctions also. Optical phenomena can be traced back to the excitation of electrons, and their subsequent return to the ground state. Thus this approach can be considered the direct simulation of the phenomena behind producing these optical properties. However there may be many different electron configurations that contribute to the generation of NLO properties. Thus, the method considers many different states, attempts to determine those that are the most important to describing the optical behavior of a molecule, and then weights these states appropriately to describe the phenomenon we are able to observe experimentally.

The SOS approach is one of the most accurate, as it directly attempts to calculate the phenomenon responsible for the properties observed. Additionally, the contribution of particular excited states to the overall observed phenomena can be deduced, allowing for a deeper understanding of the link between electronic structure and NLO properties. However, it does typically require a Configuration Interaction calculation, which is quite computationally expensive. This drastically limits the sizes of systems that can be observed, and requires a great deal of computational power. Additionally, due to the summation of many millions of states, this method is especially prone to numerical errors, such as roundoff error.

Coupled perturbed Hartree-Fock[17–19] (CPHF) is another method that can be used to compute response properties. As the name suggests, this method extends the standard Hartree-Fock method using perturbation theory. In the case of computing response properties, the perturbation parameter represents an external electromagnetic field (i.e. light). The Schrödinger equations are (approximately) solved with and without the added

perturbation. This allows one to determine how a material will behave in the presence of an electromagnetic field, and consequently, the response properties of a material.

As this method uses the Hartree-Fock formalism, it is less computationally expensive than using Configuration Interaction, since Hartree-Fock only a single electronic configuration. For most materials, the assumption of having only one configuration works reasonably well; however, this assumption may not hold true of all materials and molecules, especially those considered to be strongly correlated. Strong correlation will be discussed in more detail in further sections. Thus, CPHF may be less accurate than the SOS approach, at a lower computational cost. Additionally, the choice of basis set, convergence criteria, and grid parameters may have a drastic effect on the accuracy of the method.

Finally, Response Theory[20,21] (RT) is another perturbation theory-based method. However, this method uses a time-dependent perturbation theory approach to the Schrödinger Equation and is identical to the coupled-perturbed Hartree-Fock method when the Schrödinger equation is (approximately) solved at the Hartree-Fock level. Rather than having to compute, and sum over, a set of computationally demanding equations, in response theory only a set of coupled equations must be solved. This method is still relatively expensive, though is much cheaper than the SOS method. Currently, it is considered the standard for when using a bottom-up approach, as it combines a reasonable computational cost with high accuracy. Consequently, within this work, we use RT as the benchmark for comparing our method's numbers.

The finite-field method[22–26] takes a different approach to the aforementioned three. This method takes computed molecular energy data and attempts to fit it as the

external field is varied. The derivatives of the fitted function are then taken to determine the nonlinear optical properties as follows:

$$\begin{aligned} \mu &= E'(0) \\ \alpha &= E''(0) \\ \beta &= E'''(0) \\ \gamma &= E^{(4)}(0) \end{aligned} \qquad \text{Eq. 1.2.4}$$

One can use many different functions to fit the *E(F)* function, including Taylor polynomials, rational functions, and hypergeometric functions.

The major advantage of the finite field method is the computational cost relative to the other methods mentioned here. This method usually completes calculations in a matter of minutes, rather than days or weeks. This opens up a wide variety of possibilities, such as being able to screen large numbers of materials in a high-throughput fashion, or to look at larger systems. These applications are particularly important to the field of chemical biology, where systems are quite large, relative to those more relevant to purely traditional chemistry.

However, this method is not without its own set of drawbacks. The most apparent one is the heavy reliance of the calculation's accuracy on the parameters chosen for fitting.[27] If the fitting parameters are chosen inaccurately, the results of the finite field calculations are very inaccurate. This sensitivity has meant that: (1) Users of the method need to have experience with using the method, and have the relevant expertise, and (2) The results of the method need to have a good validation protocol. By reducing this sensitivity to chosen parameters, the reliability of this method can greatly be increased. In this work, the finite-field method is chosen as the method of choice to study NLO phenomena.

1.2.4 The Finite-Field Method

The finite field approach[22–26] is a numerical one, which takes several points at this expansion, uses them to fit an arbitrary function, and solves for the derivatives of the function as per Equation 1.2.4. As one of the advantages of this method is its cheapness, the function that is used for fitting must fulfill the following criteria: (1) The function should be easy to optimize, and (2) it should be relatively easy to determine the derivatives of this function.

In previous work, each of the finite field approaches use a polynomial as the function for fitting.[28] The polynomial model has the advantage of having the same form as the Taylor expansion that defines the NLO properties (Equation 1.2.3). Thus, solving for the coefficients in the polynomial model automatically gives one a value for the NLO properties. Additionally, to solve the coefficients of the polynomial model, a simple linear system of equations can be solved. However, the polynomial model can be quite sensitive to the field values for which the system is solved; if values are not chosen carefully, the model will not yield usable results. Additionally, there is no easy means of knowing if the results obtained are useable. This reduces the overall reliability of the method.

An alternative to using a polynomial to fit the finite field data is to use a rational model instead:

$$E(F) = \frac{a+bF+cF^2+dF^3+\cdots}{1+BF+CF^2+DF^3+\cdots} \qquad \text{Eq. 1.2.5}$$

Unlike the polynomial model, the coefficients of the rational model do not directly correspond to the NLO properties in Equation 1.2.4. However, the model is quite easy to

differentiate, as Eq. 1.2.5 can be differentiated analytically with minimal computational cost. Additionally, the rational model can also be solved using a linear system of equations, similar to the polynomial model. Thus, the rational model does not pose any significant disadvantages, in terms of computational cost, to using a polynomial fit.

However, there are many significant advantages that make the rational model a more attractive alternative to using a polynomial model. The rational model tends to have better behavior at poles and asymptotes than the polynomial model. This is quite important when fitting the energy at different external fields, as the energy is divergent with respect to the applied field. Additionally, the rational model can be thought of as a more general form of a polynomial; setting the denominator coefficients to zero yields a polynomial form. The rational model also is more robust to choices of parameters, as having the correct form tolerates more variance in choosing the correct points in the linear expansion.

The finite field method is quite computationally cheap, and can be accurate. However, the accuracy highly depends on the parameters chosen for the fitting. Choosing these parameters is the limiting factor that prevents the method from being user friendly and reliable. There are three major parameters that must be optimized for any finite field calculation: (1) The number of fields that are chosen for the calculation, (2) The spacing of the fields chosen, and (3) The starting field used for the finite field expansion. In a previous study of the polynomial method[28], the first and second factor were not difficult to chose, as they are quite forgiving to a suboptimal choice. However, the third factor is quite crucial to the accuracy of the results, and is highly unforgiving to errors in choosing it. We expect to see similar trends during studies of the rational function model.

1.3 Background of Computing Molecular Energies

1.3.1 Motivation and Relevance to NLO Property Prediction

The computation of accurate molecular energies is the central task of computational chemists. The reason why molecular energies are a staple calculation is that they are useful for calculating a variety of different properties of molecules, reactions and materials. Within the realm of quantum chemistry, there are two paradigms for the computation of molecular energy: (1) Wavefunction based methods, and (2) Density-Functional Theory (DFT) based methods. The finite field method requires the use of molecular energies at several different fields in order to create the system of equations to be solved. For this purpose, either wavefunction-based methods, or DFT-based methods can be used to obtain the energies.

These energies must be relatively accurate and have the correct trend with regards to increasing electric field strength. Otherwise, the finite field method will not produce accurate results. However, as the overarching theme of this thesis is to push the boundaries of what can be looked at with the finite field method to facilitate the routine calculation of NLO properties for biological systems, computational methods that accurately determine energies of larger systems must be considered.

The issue with computing energies of larger systems is that the trade-off between computation-time and accuracy. In general, as one increases the size of the system, the required computation power increases quickly, often as the fourth (and sometimes much, much, higher) power of the size of the system. Additionally, the more accurate the method used to compute the energy, the more computational resources are required.

Thus, to even be able to determine the energy of a larger system, one usually uses a cheap computational method, which often leads to inaccuracies in the energies computed. It has been observed that NLO properties are often exquisitely sensitive to these errors. In the following sections, we will discuss energy extrapolation methods, along with a means of refining the energy obtained through relatively cheap calculations. This is done using function fitting as well, highlighting the strong applicability of this mathematical tool to many different areas of quantum chemistry.

1.3.2 Introduction to Electronic Structure Theory Methods

Electronic structure theory based methods rely on solving the time independent Schrodinger Equation:

$$\widehat{H}\Psi(R_1, R_2 \dots R_N, r_1, r_2 \dots r_N) = E\Psi(R_1, R_2 \dots R_N, r_1, r_2 \dots r_N) \quad \text{Eq. 1.3.1}$$

This equation provides a description of the momentum and position of the electrons and nuclei in atoms and molecules. $\widehat{H}$ is the Hamiltonian operator, Ψ is the electronic and nuclear wavefunction, R_I is the position of a nucleus I, and r_i is the position of an electron, i. One of the most basic assumptions made to this equation is the Born-Oppenheimer approximation.[29] This approximation postulates that the motion of nuclei is much slower than that of electrons; this allows for the separate treatment of nuclear and electronic motion.

However, for many electron systems, the Born-Oppenheimer equation alone does not provide a tractable means of computing the energy. Thus, further assumptions must be made. The most well known one is that of the Hartree-Fock[30] method. This method simplifies the problem of computing the electron-electron repulsion by replacing a many-

body electron-electron repulsion with an average electron repulsion term instead. The main advantage to the Hartree-Fock method is that the assumption allows for the treatment of systems with many hundreds of electrons; Hartree-Fock computations for polypeptides and polynucleotides are possible, if not exactly routine. Even the energies of whole proteins have been reported in the literature using Hartree-Fock based methods.[31]

However, there are disadvantages to using the Hartree-Fock method.[30] One major disadvantage is the neglect of electron correlation, an effect of using average electronic repulsion rather than including electron-electron repulsion explicitly. This reduces the overall accuracy of the method. Additionally, the Hartree-Fock method only uses a single Slater Determinant-based wavefunction. This means that only one electron configuration may be considered in the construction of the wavefunction, but this is not necessarily a valid assumption for many systems. For example, in strongly-correlated systems multiple electron configurations make significant contributions to the energy. The accurate description of strongly-correlated systems is one of the big challenges of quantum chemistry, as these systems include, but are not limited to, superconductors and transition metal catalysts.

In order to determine the properties of strongly-correlated systems, one can use Full Configuration-Interaction (FCI).[30] This method assumes that the wavefunction can be written as a linear combination of Slater determinants. As FCI takes into account all the possible electron configurations (i.e. Slater determinants) possible, the wavefunction created is exact. However, the drawback to this method is the computational cost associated with it; FCI is only tractable for small- and medium-sized atoms and very small molecules containing only light (i.e., H-Ne) atoms.

As a compromise between FCI and HF in terms of accuracy and cost, perturbation series[32] takes a HF calculation and then and then adds systematic corrections to the energy in the form of higher order terms in the series. A user may compute as many (or as few) correctional terms as they wish. One of the most used perturbation series for computational chemistry is the Møller-Plesset (MP) perturbation series[33]. If we expand the energy of a molecule as follows:

$$E(1) = E(0) + E'(0) + \frac{1}{2!}E''(0) + \frac{1}{3!}E'''(0) + \frac{1}{4!}E^{(4)}(0) + \cdots \qquad \text{Eq. 1.3.2}$$

The function above is written in terms of a perturbation parameter, ε. The individual terms in this expansion are related to the MP series by the following relationship:

$$\begin{aligned} E(0) &= \sum_{i \in occ} \varepsilon_i \\ E'(0) &= E_{HF} - E(0) \\ E''(0) &= E_{MP2} - E_{HF} \\ E^{(n)} &= n!\,(E_{MPn} - E_{MPn-1}) \end{aligned} \qquad \text{Eq. 1.3.3}$$

The MP series terms can be computed practically to the 4th order for moderately-large organic molecules, and until the 5th order for small organic molecules. Ideally, the series will tend to converge to the "true" energy for that system as one adds terms to the energy expansion. Thus, if we can calculate a few low-order terms, use these to fit a function, and then extrapolate that fitted function to infinity, then we should potentially be able to determine this true energy.

However, this extrapolation may pose a problem, in that the MP series is well known as to diverge.[34] This means that the series does not converge to one fixed energy value as the terms in the expansion are increased. This leads to the counterintuitive notion that more computationally expensive calculations can be less accurate than less expensive ones. However, as the MP series often appears convergent at lower order, if these (non-divergent) terms are fit, we should be able to resum the series to obtain a convergent

fitting function. As with the case of the finite field approximation, many different functions can be used to fit the MP series terms. This includes polynomial and rational functions, along with even more general functions. One such example of a generalized function is the Gauss hypergeometric function. This resummation scheme will be discussed in further sections. In this thesis, resummation of the MP perturbation series is posed to be a viable method of determining accurate energies for larger systems. If one can use cheap computations for large systems, and then refine them towards the true energy, then it should be feasible to study larger systems, and especially determine NLO properties for these systems.

1.3.3 Resummation of the MP Series

As mentioned in the previous section, a perturbation series should ideally be able to converge to the true energy in the infinite limit. However, it is a well-known phenomenon that the MP series tends to diverge at terms that are higher order.[34] This usually occurs after the 4^{th}-5^{th} term in the series. Thus, lower-order terms still tend to converge towards the "true" energy value. Thus, if one could take the MP1-4 terms, and use the term values to create a convergent series that could be cheaply extrapolated to the infinite term, then one would have found a way of refining the MP series to the true energy, with minimal computational power.

In order to resum the perturbation series, a good choice would be the family of Gauss Hypergeometric functions. The general form of these functions is as follows:

$$ {}_kF_l\left(\begin{matrix}a_1,\dots,a_k\\ b_1,\dots,b_l\\ c\end{matrix}\right) = \sum_{n=0}^{\infty}\frac{(a_1)_n\dots(a_k)_n}{(b_1)_n\dots(b_l)_n}(cx)^n \qquad \text{Eq. 1.3.4} $$

where the Pochammer symbols are defined by gamma functions (Γ) as follows:

$$(a)_n = \frac{\Gamma(a+n)}{\Gamma(a)} \qquad \text{Eq. 1.3.5}$$

Through this expansion, it becomes apparent that the structure of these functions is combinatoric in nature. Though they seem complicated at first glance, these functions present several attractive features that make them a good fit for a problem of this nature.

The features that make these functions attractive include their ability to exactly describe many different families of functions including geometric, logarithmic, elliptic, exponential, and many different types of (associated) orthogonal polynomials. Additionally, there are several mathematical tricks that are available that can help with the practical application of hypergeometric functions. Currently, the issue with optimization of nonlinear functions like these is that convergence is quite difficult to achieve. Having explicit mathematical identities to exploit can be very helpful because it allows one to (partially) optimize the systems of equations explicitly.[35]

To resum the perturbation series, we note that we can truncate the energy expansion in Equation 1.3.2 to four terms:

$$E(1) \approx E(0) + E'(0) + \frac{1}{2!}E''(0) + \frac{1}{3!}E'''(0) + \frac{1}{4!}E^{(4)}(0) \qquad \text{Eq. 1.2.6}$$

We can then normalize this series by dividing each of the terms by *E(0)*. If we define each of our terms in series 1.2.6 as $O_n = \delta o_n U^n$, where n represents the n-th term, to be defined as, we can rewrite our normalized series in the following way:

$$E(1) = 1 + \delta o_1 U + \frac{1}{2!}\delta o_2 U^2 + \frac{1}{3!}\delta o_3 U^3 + \frac{1}{4!}\delta o_4 U^4 \qquad \text{Eq. 1.2.7}$$

Then, we note that we can set the third parameter in the hypergeometric equation (Equation 1.3.4) to $c = cU$. Finally, each of the respective four terms can be equated to form a system of nonlinear equations, as follows:

$$\delta o_n = \frac{(a_1)_n (a_2)_n \ldots}{(b_1)_n} (cx)^n \quad \text{Eq. 1.2.8}$$

Where we take n=1, 2,3,4 to create the system of equations. Note that the form used above is the $_2F_1$ Gauss Hypergeometric, but if more terms are calculated, then one can use a $_2F_2$ (or higher) Hypergeometric function.

This system of nonlinear equations must be solved, to get our coefficients $(a_1)_n, (a_2)_n, (b_1)_n, c$. This solution should provide us with a convergent hypergeometric function, that we can then solve at U=1. That would give us the value of the MPn series if we were to apply an infinite order correction to it.

One note about solving the nonlinear equations is that there is no explicit formula known to solve this system of equations. If we were only looking at the even order terms, however, there are means of solving the system with diagonal Pade approximants.[35] The case with even order terms does come up in some contexts for our overall problem. However, if we assume there is no explicit formula, then we must use a nonlinear system solver. In our case, we choose to use the scipy.optimize Python package, as it is a simple, yet sufficiently robust, solver for problems of this type.

1.4 Future Directions

1.4.1 Motivation

As the overall project progressed, it became apparent that we were not able to further use more complex nonlinear functions due to issues with optimization. This became apparent when attempting to use hypergeometric functions in NLO property prediction, as discussed in the following section. Thus, future directions of this project

would need to satisfy two criteria: (1) Functions that are easy to optimize, while (2) increasing the flexibility of fitting, to allow for more accurate fits. For example, the using the Meijer-G family of functions provides a promising alternative to solving systems of nonlinear equations with hypergeometric functions.[36] This scheme is detailed in the following section. This function fitting may be promising in other areas of quantum chemistry as well, including such as Density Functional Theory.

Although we looked at NLO property prediction in this thesis, we only have looked at property prediction along a singe axis. To generalize to more real systems, we need to include the y- and z-axis to determine these properties in three dimensions. As the finite field method worked well for the single axis case, it is a logical choice for the three-dimensional case as well. This forms a key direction for future work on this method.

1.4.2 Hypergeometric Functions for NLO Property Prediction

To use hypergeometric functions with the finite-field method[22–26], one replaces the Taylor polynomial in traditional methods with a hypergeometric function instead. This means that the linear systems of equations that arises with the polynomial and rational models is no longer valid. Thus, a nonlinear solver must be used to determine the coefficients for the hypergeometric model. However, solving the function, and determining derivatives is a trivial exercise, as the function's series form lends itself well to this.

In our work, we used Covariance Matrix Adaptation Evolution Strategy (CMA-ES)[37] to optimize the system of nonlinear equations. One advantage to using a nonlinear solver such as CMA-ES is that one can use as many points as desired to optimize the

function. However, this is not necessarily practical from a computational cost standpoint, as one of the main draws of the finite-field method is that it is computationally cheap to use. Despite this, the flexibility to use as many, or as little points for fitting creates an additional layer of flexibility that may help with how well the function fits. This is in contrast to the rational model, which only could use as many points as dictated by the truncated form of the function.

1.4.3 Moving Beyond Hypergeometric Resummation

Although the hypergeometric function does provide a high degree of flexibility in fitting different functions, one of the major drawbacks of employing it is the issue with optimizing the system of nonlinear equations that tends to result. These issues are quite prevalent when dealing with systems of nonlinear equations that are complex. The Meijer-G resummation method[36] seems to be a promising method to circumvent this issue. If we take a series of the form:

$$Z(g) = \sum_{n=0}^{\infty} z_n g^n \qquad \text{Eq. 1.4.1}$$

where $z_0 = 1$ (i.e. the series is normalized). This method takes four different steps to implement. The first step is to regularize the series to be fitted by making a Borel transform of the coefficients, which is simply dividing our series in Equation 1.4.1 with:

$$b_n = \frac{z_n}{n!} \qquad \text{Eq. 1.4.2}$$

Next, we take the ratios of consecutive Borel (b_n) coefficients:

$$r_N(n) = \frac{b_{n+1}}{b_n} \qquad \text{Eq. 1.4.3}$$

We can then make the assumption that the ratios of the coefficients can be approximated via the rational function defined as:

$$r_N(n) = \frac{\sum_m^l p_m n^m}{1+\sum_{m=1}^l q_m n^m} \quad \text{Eq. 1.4.4}$$

We then solve the resultant system of equations to create solutions vectors in the form:

$$\begin{matrix} \sum_{m=0}^l p_m x^m = 0 \\ \sum_{m=1}^l q_m y^m = 0 \end{matrix} \quad \text{Eq. 1.4.5}$$

These solutions vectors uniquely determine a hypergeometric equation. We can finally get back our resumed equation by solving the following equation:

$$O_{B,N}(g) = \frac{\prod_{i=1}^l \Gamma(-y_i)}{\prod_{i=1}^l \Gamma(-x_i)} G_{l+1,l+2}^{l+2,1}\left(\begin{matrix} 1, -y_1, \dots, -y_l \\ 1, 1, -x_1, \dots, -x_l \end{matrix} \middle| -\frac{q_l}{p_l g}\right) \quad \text{Eq. 1.4.6}$$

Where the *G* function is the Meijer-G function. The resultant sum gives us an (approximate) resummation of the divergent series. This method looks to be quite promising to increase reliability of the hypergeometric resummation method for the MP series, while maintaining the flexibility of the generalized functions.

1.5 References

(1) Franken, P. A.; Hill, A. E.; Peters, C. W.; Weinreich, G. Generation of Optical Harmonics. *Phys. Rev. Lett.* **1961**, *7*, 118–119.

(2) Nalwa, H. S.; Miyata, S. *Nonlinear Optics of Organic Molecules and Polymers*; CRC Press, 1997.

(3) Brédas, J. L.; Adant, C.; Tackx, P.; Persoons, A.; Pierce, B. M. Third-Order Nonlinear Optical Response in Organic Materials: Theoretical and Experimental Aspects. *Chem Rev* **1994**, *94*, 243–278.

(4) Luo, Y.; Ågren, H.; Jørgensen, P.; Mikkelsen, K. V. Response Theory and Calculations of Molecular Hyperpolarizabilities. *Adv. Quantum Chem.* **1995**, *26*, 165–237.

(5) Denk, W.; Strickler, J. H.; Webb, W. W. Two-Photon Laser Scanning Fluorescence Microscopy. *Science* **1990**, *248*, 73–76.

(6) Albota, M.; Beljonne, D.; Bredas, J. L.; Ehrlich, J. E.; Fu, J. Y.; Heikal, A. A.; Hess, S. E.; Kogej, T.; Levin, M. D.; Marder, S. R.; et al. Design of Organic Molecules with Large Two-Photon Absorption Cross Sections. *Science (80-.).* **1998**, *281*, 1653–1656.

(7) Bloembergen, N. Nonlinear Optics. In *Nonlinear Optics*; 1996.

(8) Born, M. *Optik*; Springer Berlin Heidelberg: Berlin, Heidelberg, 1933.

(9) Korff, S. A.; Breit, G. Optical Dispersion. *Rev. Mod. Phys.* **1932**, *4*, 471–503.

(10) Clays, K.; Persoons, A. Hyper-Rayleigh Scattering in Solution. *Phys. Rev. Lett.* **1991**, *66*, 2980–2983.

(11) Clays, K.; Persoons, A. Hyper-Rayleigh Scattering in Solution. *Rev. Sci. Instrum.* **1992**, *63*, 3285–3289.

(12) Levine, B. F.; Bethea, C. G. Second and Third Order Hyperpolarizabilities of Organic Molecules. *J. Chem. Phys.* **1975**, *63*, 2666–2682.

(13) Felker, P. M.; Zewail, A. H. Purely Rotational Coherence Effect and Time-resolved sub-Doppler Spectroscopy of Large Molecules. I. Theoretical. *J. Chem. Phys.* **1987**, *86*, 2460–2482.

(14) Ditchfield, R.; Ostlund, N. S.; Murrell, J. N.; Turpin, M. A. Comparison of the Sum-over-States and Finite Perturbation Theories of Electrical Polarizability and Nuclear Spin-Spin Coupling. *Mol. Phys.* **1970**, *18*, 433–440.

(15) Meyers, F.; Marder, S. R.; Pierce, B. M.; Brédas, J. L. Electric Field Modulated Nonlinear Optical Properties of Donor-Acceptor Polyenes: Sum-Over-States Investigation of the Relationship between Molecular Polarizabilities (A,β, and Γ.) and Bond Length Alternation. *J. Am. Chem. Soc.* **1994**, *116*, 10703–10714.

(16) Champagne, B.; Kirtman, B. Evaluation of Alternative Sum-over-States Expressions for the First Hyperpolarizability of Push-Pull π-Conjugated Systems. *J. Chem. Phys.* **2006**, *125*, 24101.

(17) Stevens, R. M.; Pitzer, R. M.; Lipscomb, W. N. Perturbed Hartree—Fock Calculations. I. Magnetic Susceptibility and Shielding in the LiH Molecule. *J. Chem. Phys.* **1963**, *38*, 550–560.

(18) Gerratt, J.; Mills, I. M. Force Constants and Dipole-Moment Derivatives of Molecules from Perturbed Hartree–Fock Calculations. II. Applications to Limited Basis-Set SCF–MO Wavefunctions. *J. Chem. Phys.* **1968**, *49*, 1730–1739.

(19) Caves, T. C.; Karplus, M. Perturbed Hartree–Fock Theory. I. Diagrammatic

Double-Perturbation Analysis. *J. Chem. Phys.* **1969**, *50*, 3649–3661.

(20) Helgaker, T.; Coriani, S.; Jørgensen, P.; Kristensen, K.; Olsen, J.; Ruud, K. Recent Advances in Wave Function-Based Methods of Molecular-Property Calculations. *Chem. Rev.* **2012**, *112*, 543–631.

(21) Jansik, B.; Sałek, P.; Jonsson, D.; Vahtras, O.; Ågren, H. Cubic Response Functions in Time-Dependent Density Functional Theory. *J. Chem. Phys.* **2005**, *122*, 54107.

(22) Cohen, H. D.; Roothaan, C. C. J. Electric Dipole Polarizability of Atoms by the Hartree—Fock Method. I. Theory for Closed-Shell Systems. *J. Chem. Phys.* **1965**, *43*, S34–S39.

(23) Maroulis, G.; Bishop, D. M. On the Dipole and Higher Polarizabilities of Ne(1S). *Chem. Phys. Lett.* **1985**, *114*, 182–186.

(24) Maroulis, G.; Thakkar, A. J. Multipole Moments, Polarizabilities, and Hyperpolarizabilities for N_2 from Fourth-order Many-body Perturbation Theory Calculations. *J. Chem. Phys.* **1988**, *88*, 7623–7632.

(25) Bishop, D. M.; Pipin, J.; Lam, B. Field and Field-Gradient Polarizabilities of BeH, BH and CH^+. *Chem. Phys. Lett.* **1986**, *127*, 377–380.

(26) Bishop, D. M.; Pipin, J. Field and Field-Gradient Polarizabilities of H_2O. *Theor. Chim. Acta* **1987**, *71*, 247–253.

(27) Patel, A. H. G.; Mohammed, A. A. K.; Limacher, P. A.; Ayers, P. W. Finite Field Method for Nonlinear Optical Property Prediction Using Rational Function Approximants. *J. Phys. Chem. A* **2017**, *121*, 5313–5323.

(28) Mohammed, A. A. K.; Limacher, P. A.; Champagne, B. Finding Optimal Finite Field Strengths Allowing for a Maximum of Precision in the Calculation of Polarizabilities and Hyperpolarizabilities. *J. Comput. Chem.* **2013**, *34*, 1497–1507.

(29) Born, M.; Oppenheimer, J. R. Born-Oppenheimer Approximation. *Ann. Phys.* **1927**, *84*, 457.

(30) Szabo, A.; Ostlund, N. S. Modern Quantum Chemistry: Introduction to Advanced Electronic Structure Theory. *Introduction to Advanced Electronic Structure Theory*. 1982.

(31) He, X.; Merz, K. M. Divide and Conquer Hartree−Fock Calculations on Proteins. *J. Chem. Theory Comput.* **2010**, *6*, 405–411.

(32) Cramer, C. J. *Essentials of Computational Chemistry : Theories and Models*;

Wiley, 2004.

(33) Møller, C.; Plesset, M. S. Note on an Approximation Treatment for Many-Electron Systems. *Phys. Rev.* **1934**, *46*, 618–622.

(34) Olsen, J.; Jørgensen, P.; Helgaker, T.; Christiansen, O. Divergence in Møller–Plesset Theory: A Simple Explanation Based on a Two-State Model. *J. Chem. Phys.* **2000**, *112*, 9736.

(35) Mera, H.; Pedersen, T. G.; Nikolić, B. K. Hypergeometric Resummation of Self-Consistent Sunset Diagrams for Steady-State Electron-Boson Quantum Many-Body Systems out of Equilibrium. *Phys. Rev. B* **2016**, *94*, 165429.

(36) Mera, H.; Pedersen, T. G.; Nikolić, B. K. Fast Summation of Divergent Series and Resurgent Transseries from Meijer- G Approximants. *Phys. Rev. D* **2018**, *97*.

(37) Hansen, N.; Ostermeier, A. Completely Derandomized Self-Adaptation in Evolution Strategies. *Evolutionary computation*. 2001, pp 159–195.

Chapter 2

Finite Field Method for Nonlinear Optical Property Prediction Using Rational Function Approximants*

2.1 Motivation

This chapter investigates a novel method of computing NLO properties, in the form of a rational function based finite field method. Though the finite field method is quite accurate, it is not very robust to the choices of electric fields one uses for the computation of NLO properties. Thus, we hypothesized that using a function that fits the

*Work published as: Patel, A. H. G.; Mohammed, A. A. K.; Limacher, P. A.; Ayers, P. W. Finite Field Method for Nonlinear Optical Property Prediction Using Rational Function Approximants. *J. Phys. Chem. A* **2017**, *121*, 5313–5323.

energy with respect to a field (E(F)) more closely would help with the accuracy of the finite field method, and increase the overall robustness. This should help this method be more useful for uses in pharmaceutical and biomaterials development, as increased robustness would translate to less user intervention needed, allowing for more widespread use by those not necessarily experienced in doing calculations of this nature.

2.2 Introduction

Since the discovery of nonlinear optical (NLO) phenomena[1] and their uses, determining response polarizabilities and hyperpolarizabilities for molecules and polymers has become increasingly relevant to many fields, including materials science and organic chemistry[2]. Consequently, the demand for cheap and accurate computational methods to predict these molecular properties has increased.[3,4] However, producing a method that achieves these goals is challenging, as the (hyper)polarizabilities are higher-order derivatives of a molecule's energy with respect to an external homogeneous electric field (F), as follows:

$$E(F) = E(0) + \left.\frac{\partial E}{\partial F}\right|_0 F + \frac{1}{2!}\left.\frac{\partial^2 E}{\partial F^2}\right|_0 F^2 + \frac{1}{3!}\left.\frac{\partial^3 E}{\partial F^3}\right|_0 F^3 + \frac{1}{4!}\left.\frac{\partial^4 E}{\partial F^4}\right|_0 F^4 + \cdots \qquad \text{Eq. 2.1}$$

The dipole moment (μ), the dipole polarizability (α), the first hyperpolarizability (β) and the second hyperpolarizability (γ) can be substituted in the expansion:

$$E(F) = E(0) - \mu F - \frac{1}{2}\alpha F^2 - \frac{1}{6}\beta F^3 - \frac{1}{24}\gamma F^4 + \cdots \qquad \text{Eq. 2.2}$$

Several approaches are available to compute these NLO properties, including: sum over states[5], coupled-perturbed Hartree-Fock (HF)[6–8], response theory[9,10], and the finite field (FF) method[11–15]. Of these, the FF method remains one of the most computationally inexpensive, since unlike the other methods, no excited state information

or analytical derivatives are required.[16] This also makes the FF method one of the most facile to implement; simply knowing the energy at several field strengths is sufficient to compute a desired optical property. For these reasons, the FF method is commonly used first when one wishes to assess the performance of new quantum chemistry methods for (hyper)polarizabilities.[17–29]

Though the FF method has many advantages, the accuracy of a FF calculation is highly sensitive to the fields used. This sensitivity originates from the errors caused by choosing field strengths that are too high or low. The numerical nature of the FF method implies that choosing field strengths that are too low will cause finite-precision artefacts. Conversely, fields that are too high make higher-order terms in Eq. (2.1) nonnegligible, leading to errors when the Taylor series is truncated. When there are low-lying excited states, using fields that are too high can lead to a field-induced state inversion, where an excited state at zero-field becomes lower in energy than the ground state.[30] This leads to properties being evaluated for the more favourable excited state rather than for the ground state, as desired. As a consequence of these effects, chosen field strengths must be optimized to ensure that computed (hyper)polarizabilities are accurate.

In previous work, it was found that three factors play a key role in the accuracy of a FF method: the total number of fields used, the distribution of the fields, and the initial field value around which the other fields are picked.[31] This previous study tuned these three factors for a Taylor expansion based FF method.[31] In particular, this previous method was based on taking finite differences, using a Taylor polynomial, to compute NLO properties. The optimized method, in conjunction with iterative error reduction using Richardson extrapolation, was found to provide accurate predictions for NLO

properties. However, the accuracy of this method was found to be quite sensitive to the initial field used for the calculation. This sensitivity tends to reduce the overall reliability of the method, creating a significant barrier to its widespread adoption and use.

To mitigate the field sensitivity observed with the finite difference method, we propose using a rational function to fit the energy instead:

$$E(F) = \frac{a+bF+cF^2+dF^3+\cdots}{1+BF+CF^2+DF^3+\cdots} \quad \text{Eq. 2.3}$$

Where a, b, c, d,… and B, C, D,… are fitting coefficients. By setting all the denominator coefficients to zero, a polynomial is obtained, so this function is a generalized form of the Taylor expansion. However, rational functions are well-suited to approximate asymptotic functions and, recalling their use in Padé approximants, (approximately) account for higher-order terms in the Taylor series (Eq. 2.1), as one must do especially for larger fields. We hypothesized that these properties of rational functions may allow for improvement in the energy fitting procedure. Consequently, the overall error in a FF calculation might be reduced, which would increase the range of electric fields that produce an acceptable error. To test this hypothesis, in this work, a rational function based FF method is optimized and compared to the Taylor FF method.

As in our previous work on the Taylor, or polynomial, FF model[31], three factors vital to the accuracy of the rational FF model will be optimized in this study. First, the ideal number of terms for the rational function approximant will be determined, which gives the number of fields used in the calculation. Then, different distributions of the chosen fields will be tested, in order to determine which distributions allow for the most accurate calculation of NLO properties. Finally, the error dependence on initial field strengths for various molecules is explored. If any trends are present, they will be used to

produce an algorithm that can choose initial fields optimally. After the rational-function FF method is optimized, its accuracy and behaviour in calculating response properties shall be compared to the previous polynomial-based method.

2.3 Methods

2.3.1 Overview of the Rational Function Approximation for the FF method

To produce enough data points for the FF approximation, the energy of a molecule must initially be solved for at various field strengths. Selecting the appropriate field strengths begins with choosing an initial field strength (F_0), around which the other chosen field strengths (F) are distributed. For this variant of the FF method, the selected fields are distributed according to:

$$F_{\square} = x^n F_0 \qquad \text{Eq. 2.4}$$

In this study, $x = 2^{\frac{p}{100}}$ and $F_0 = F_{min} \times 2^{\frac{j}{100}}$. Substituting these forms into Equation (4) produces:

$$F_n = \left(2^{\frac{p}{100}n}\right)\left(F_{min} \times 2^{\frac{j}{100}}\right) = F_{min} \times 2^{\frac{(j+pn)}{100}} \qquad \text{Eq. 2.5}$$

Where j is any integer between 1-800, p is any integer between 1-100, and $F_{min} = 0.0005\, a.u.$ For N unknown coefficients in the rational function (Equation 3), $\left\{n \in \mathbb{Z}^* | 0 \leq n \leq \left(\frac{N}{2} - 1\right)\right\}$ for even values of N, and $\left\{n \in \mathbb{Z}^* | 0 \leq n \leq \left(\frac{N-3}{2}\right)\right\}$ for odd values of N. In addition, for both even and odd values of N, the energy at $F = 0$ is also determined, since this simplifies Equation 2.3 to:

$$E(0) = a, \qquad \text{Eq. 2.6}$$

allowing for a to be determined directly. To determine the remaining coefficients, each F_n value is substituted into Equation 2.3. Since both $+F_n$ and $-F_n$ are used, each F_n value produces two equations. These substituted equations can be rearranged into the form:

$$\begin{gathered} E(F_0) + BF\big(E(F_0)\big) = a + F_0 b + {F_0}^2 c \\ E(-F_0) - B(F_0\big(\square(-F_0)\big) = a - F_0 b + {F_0}^2 c \\ E(xF_0) + BxF_0\big(E(xF_0)\big) = a + xF_0 b + x^2 {F_0}^2 c \\ E(-xF_0) - BxF_0\big(E(-xF_0)\big) = a - xF_0 b + x^2 {F_0}^2 c \\ \vdots \end{gathered} \qquad \text{Eq. 2.7}$$

By substituting $E(0) = a$, and rearranging into the form $A\vec{x} = \overrightarrow{\square}$:

$$\begin{bmatrix} -F(E(F)) & F & F^2 \\ F(E(-F) & -F & F^2 \\ -xF(E(xF)) & xF & x^2F^2 \\ xF(E(-xF)) & -xF & x^2F^2 \end{bmatrix} \begin{bmatrix} B \\ b \\ c \end{bmatrix} = \begin{bmatrix} E(F) - E(0) \\ E(-F) - E(0) \\ E(xF) - E(0) \\ E(-xF) - E(0) \end{bmatrix} \qquad \text{Eq. 2.8}$$

Since both the positive and negative fields are used, for even values of N the system is overdetermined. This overdetermined system can be solved through least squares, or by discarding one of the equations. Both approaches are discussed further in Section 2.3.3.

Once the coefficients for Equation (3) are determined by solving the system of equations 2.8, the response properties can then be determined by taking the appropriate derivatives of Equation 2.3 at $F = 0$:

$$\begin{gathered} \mu = -E'(0) \\ \alpha = -E''(0) \\ \beta = -E'''(0) \\ \gamma = -E^{(4)}(0) \end{gathered} \qquad \text{Eq. 2.9}$$

2.3.2 Optimizing the rational function form and field distribution

Using the general method presented in Section 2.3.1, the energies of five randomly selected molecules were fit by rational functions with various numbers of numerator and denominator terms (Table 2.1). The molecules tested were: acetamide, 4-amino-4'-nitrobiphenyl (DPAN), 1-hexadecanol, hexa-1,3,5-triene (PA3), and 1-amino-10-nitro-deca-1,3,5,7,9-pentaene (PA5AN). For each molecule, plots comparing the error in computed properties (α, β, γ) over varying p and F_0 (Equations 2.4 and 2.5) were generated for each approximant form (Figures 2.1 and 2.2). For more information on benchmark values and error calculation, refer to Section 2.3.5.

Table 2.1. The forms of the rational function benchmarked for their accuracy in fitting molecular energies.

Model number	Numerator degree	Denominator degree
1	3	2
2	4	3
3	4	4
4	2	2
5	3	3

These plots were used to fix the form of the rational function as model 2 for the remainder of the study. The form of model 2 is:

$$E(F) = \frac{a+bF+cF^2+dF^3}{1+BF+CF^2} \qquad \text{Eq. 2.10}$$

Since this model has four terms in the numerator and three terms in the denominator, each further FF calculation requires the molecular energy at five nonzero field values, along with the molecular energy at $F = 0$. This is not surprising, since for a fixed (but large) basis set, one expects the energy to diverge to minus infinity linearly with F in the high-field limit.

Having determined the optimal functional form for the rational function, the generated plots were also used to fix the value of $p = 50$ for Equation (5). This corresponds to a common ratio of $x = \sqrt{2}$ for the geometric progression used to distribute fields in Equation (4) and it is the same ratio that we found when investigating the polynomial form in ref. 31.

2.3.3 Testing the least squares solution

The form of the rational function given by model 2 (Equation 2.10) contains six unknown coefficients, one of which can be determined directly using Equation 2.6. For the remaining five unknown coefficients, positive and negative fields are picked using Equation 2.5. Thus, six equations were generated for five unknowns in this case, leading to an overdetermined system. To ensure that solving the system using least squares provides a consistently accurate result relative to discarding one of the equations, the error in computed response properties over varying F_0 values was plotted for both approaches. An example plot for acetamide is given in Figure 2.3. Using these plots, it was determined that least squares provided an adequate solution to the overdetermined system. Thus, for the remainder of the study, the least squares solution to Equation 2.8 was used. To obtain solutions to both the overdetermined and truncated system of equations, the linear systems were solved using the numpy.linalg Python package.

2.3.4 Developing a protocol to find optimal values of F_0

For FF methods, picking the optimal F_0value is crucial in ensuring the computed response properties are accurate.[31] However, the optimal F_0 drastically varies for each NLO property calculation. Thus, we devised an automatic method to determine an adequate F_0 value. This F_0 picking method arises from the investigation conducted in Section 2.3.3, as it uses the property values calculated by either least squares or truncating the system of equations (Equation 8). In particular, the difference between the truncated solutions from the least squares solution is used to produce an indicator, denoted as r:

$$r = \frac{(q_{max} - q_{min})}{q_{regression}} \quad \text{Eq. 2.11}$$

Where $q = \alpha, \beta, \gamma,$ and max and min are the maximum and minimum values of the properties calculated by removing one of six equations, respectively. Additionally, $regression$ refers to the value of the properties computed using least squares. The quantity r can be thought of as an error metric that is the ratio between (a) the difference between the maximum and minimum values of q obtained when the equations are solved using leave-one-out analysis and (b) the predicted property value obtained by least-squares solution on the complete dataset.

In total, this procedure requires seven points for each F_0 value to generate the corresponding r value. A representative plot comparing γ values calculated via the two methods of solving Equation 2.8 is given in Figure 2.4a. Additionally, an example of the r value plotted with respect to F_0 is given in Figure 2.4b.

To pick an F_0 value that minimizes the error in a calculated property, the r value was observed as the F_0 value is increased. Starting from the low-field limit, the first F_0 value for which the r value increases or decreases for five consecutive F_0 values was

taken as the F_0 used for the FF calculation. The F_0 chosen in this manner was used to calculate α and γ for a set of 121 molecules (Figure 2.5), and β for a set of 91 molecules (Figure 2.6).

2.3.5 Electronic structure calculations and reference values to determine errors

All energy calculations in this study were performed using DALTON 2.0.[32] The level of theory used was Hartree-Fock, with a 6-31G* basis set[33]. For the calculation of electric properties, the HF method was found to be superior to conventional DFT.[34,35] All molecular geometries were optimized with this level of theory and basis set prior to computing the energy. The reference values for the α, β and γ properties were calculated using response theory (RT).[9,10] These RT values were used to calculate the error (ε) in a given response property using the following formula:

$$\varepsilon_{\alpha,\beta,\gamma} = \left|\frac{\alpha,\beta,\gamma_{calc}}{\alpha,\beta,\gamma_{RT}} - 1\right| \qquad \text{Eq. 2.12}$$

Where $\alpha, \beta, \gamma_{calc}$ is the response property computed using the rational-function FF method, and $\alpha, \beta, \gamma_{RT}$ is the corresponding property computed using RT. To ensure that the reference values computed by RT were accurate enough to compare to the properties computed using the FF method, the convergence criteria for α_{RT} was 10 significant figures or greater, and for β_{RT} and γ_{RT}, nine and eight significant digits, respectively.

Since assessing the finite field method requires the comparison of many similar and small numbers, issues related to numerical precision can become quite significant. Thus, all wave functions and molecular energies were tightly converged. All the energies

used in this study are exact to at least 2e-12 a.u. Since the smallest molecules in this study have absolute energies above 40 a.u., this leads to a relative precision of 1e-13 a.u. for the energy, corresponding to 13 significant digits.

2.4 Results and Discussion

2.4.1 Determining the optimal form of the rational function to fit the energy

Observing the plots for computing γ for acetamide in Figure 1, the accuracy and overall behaviour of the truncated rational functions (Table 2.1) were compared. Models 1 and 4 can immediately be excluded from consideration, due to their relative lack of accuracy. Moreover, for model 3, the two blue bands signifying a double minima preclude it from being considered further; the presence of more than one minimum makes it difficult to optimally choose both the initial field and field distribution. Finally, a comparison between models 2 and 5 reveals that the minimum of model 5 is not as well defined when compared to model 2. This is supported by the diffuse blue band observed in the model 5 plot, which contrasts with the better-defined blue band in the model 2 plot. Overall, model 2 was found to have the best accuracy, while retaining desirable error behaviour. A similar analysis was performed with the graphs generated for the remaining test molecules and NLO properties; the behaviour and accuracy of model 2 was generally found to hold for these as well. Thus, for the remainder of the study, the form of the rational function used was model 2 (Equation 2.10).

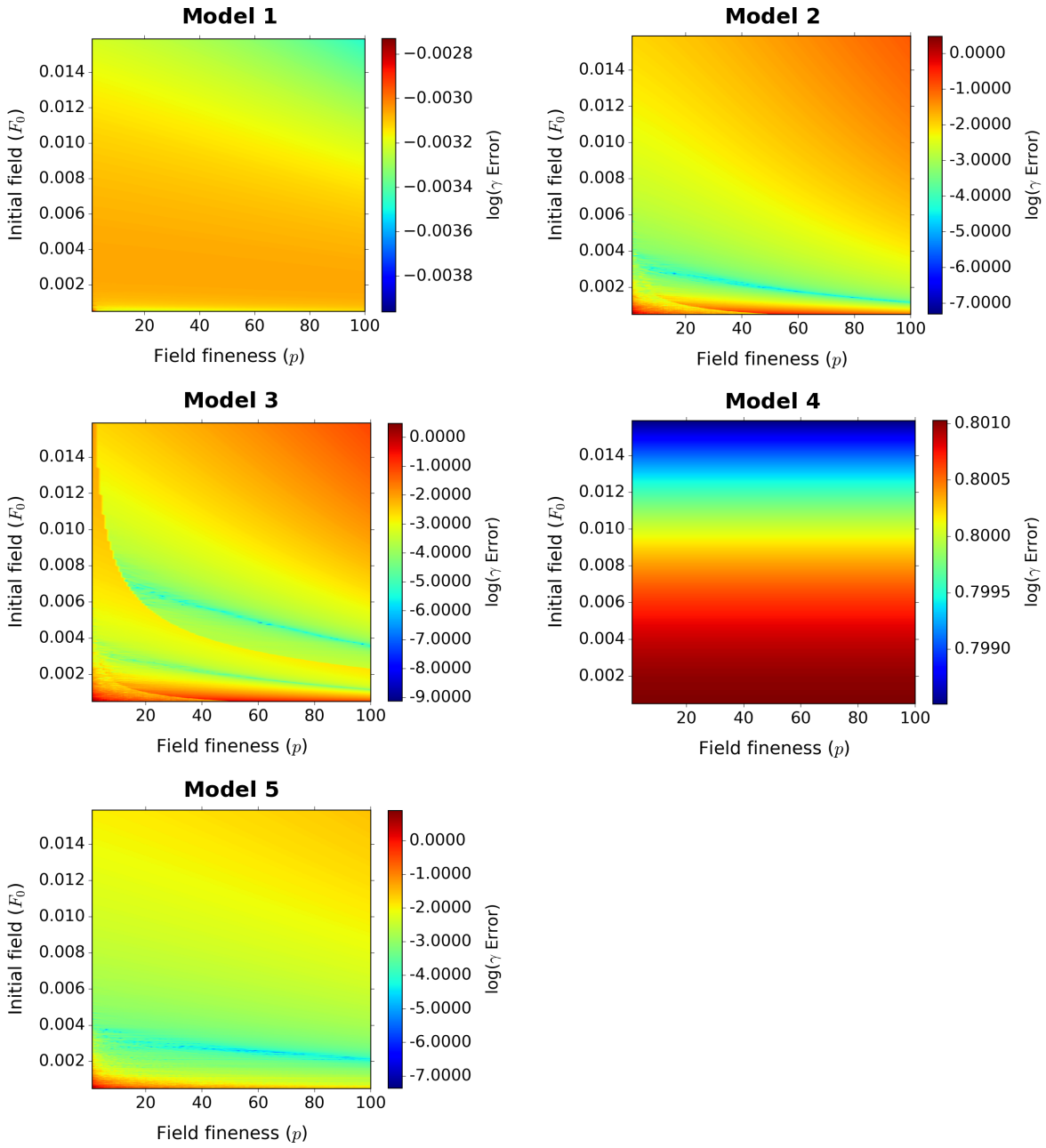

Figure 2.1. The behaviour of different rational function models in computing γ for acetamide. For each rational function form, the error relative to the reference value was determined as the initial field (F_0) and the field fineness (p) were changed. Model 2 was chosen as the best form of the rational function, since its plot contains a relatively tight and continuous blue band. This band indicates a desirable error distribution, along with low overall errors. The corresponding α and β plots for acetamide confirmed that model 2 should be used. The analysis was repeated with four additional molecules: 4,4-nitrophenyl aniline (DPAN), hexadecanol, 3-subunit polyacetylene (PA3), and 5-unit polyacetylene aminonitro (PA5AN). This confirmed the trends observed for acetamide.

2.4.2 Optimizing the field distribution parameters

Once the form of the rational function was fixed to model 2, the following step is to optimize the field distribution for the FF calculations. For the previous polynomial based FF method[31], the field distribution was found to be important for the accuracy of the method. In particular, using a geometric progression with a common ratio of $\sqrt{2}$ was found to produce the most accurate NLO property values. Thus, in this study, we also choose to distribute the fields according to a geometric progression (Equation 4). The common ratio of this progression, denoted by x, is expanded as $x = 2^{\frac{p}{100}}$. Through varying the value of p from 1-100, the interspacing between chosen fields can be tuned. The effect of varying the p value on the accuracy of the method was observed using plots such as those in Figure 2.2. Though only the plots for γ are shown for the five test molecules (Methods, Section 2.2), the plots for α and β were found to show the same trends as those observed for γ.

As predicted, the plots in Figure 2.2 demonstrate dependence between the accuracy in γ and the value of p picked for a calculation. However, since the bands corresponding to the minimal error span a large range of p values for the molecules, this implies that the value of p does not have to be picked precisely. For all five molecules, the minimal error band appears for values of p between 20-60. Though any value between these will work equally well, the remainder of the study fixed $p = 50$, producing a common ratio of $x = \sqrt{2}$. This optimal common ratio was found to be the same as that observed for the polynomial based FF method.[31]

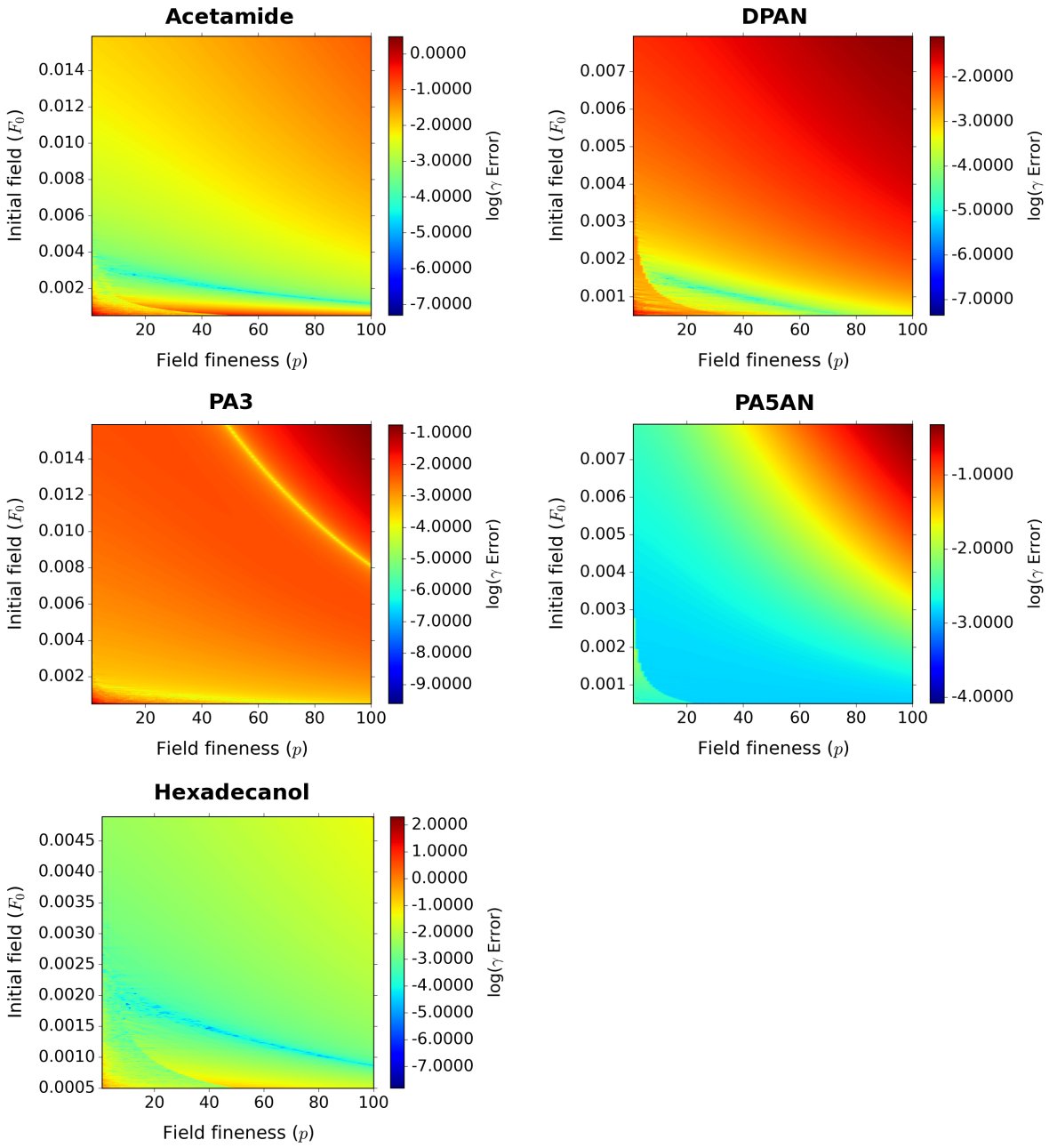

Figure 2.2. Contour plots of the error in γ for five test molecules to determine the optimal field fineness (p) value. The bands corresponding to minimal error are bright blue, except for PA3, where it is yellow. These error bands are present for every molecule from p = 20-60. The error within these bands is stable, indicating that any choice of p between 20-60 will be equally valid. Thus, the value of p was fixed to 50 for the remainder of the study.

2.4.3 Testing the least squares solution

For the rational function form given in Equation 10, there are six equations in five unknowns, i.e. the system is overdetermined. This system was solved by either least squares or truncating the system through removing one equation. Figure 2.3, where errors in γ are computed for acetamide, gives a representative example of a plot used to assess the accuracy of both methods.

At lower fields, the accuracy of the least squares solution and the solutions obtained through leaving an equation out are similar. Depending on which equation was removed, the F_0 at which the error is minimized varies, with no discernable pattern. At higher fields, all solutions show similar behaviour, but have varying errors. One observed trend is that the solution obtained by removing the first equation from the system given in Equation 2.8 is generally very similar in behaviour and accuracy to the least squares solution. This suggests that the equations constructed with low field strengths contain less information than those using higher fields.

Though the solution obtained through removing the first equation showed predictable behaviour relative to the least squares solution, this did not hold true for the rest of the equations. By leaving an equation out of the system of equations 2.8, the error could increase or decrease, with no clear trends indicating which equations would lower the error when removed. Thus, as the least squares solution performed most predictably with regards to accuracy and behaviour, it was used for the remainder of the study.

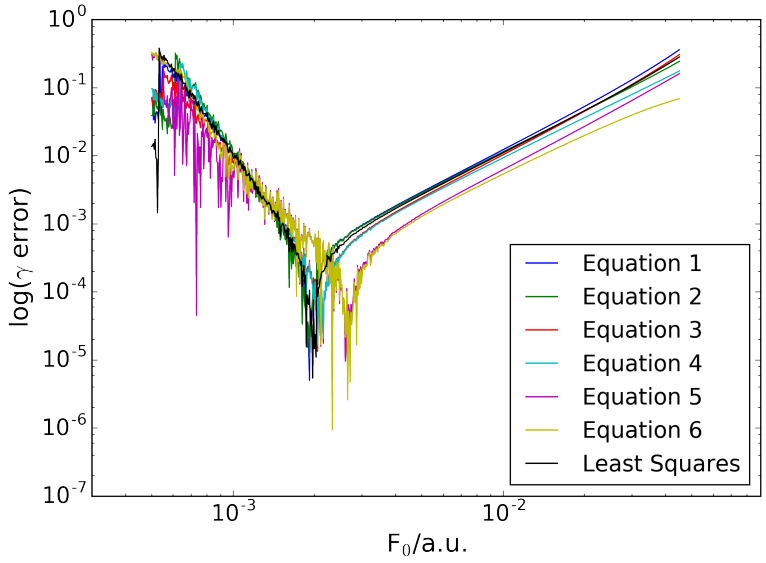

Figure 2.3. Example of a plot used to assess the performance of the least squares solution compared to solving a truncated system of equations. Here, the errors in computing γ for acetamide using model 2 are shown. No consistent trends between the least squares and truncated solutions could be found between molecules and properties. Thus, the least squares solution was used for the remainder of the study.

2.4.4 Determining optimal initial fields for FF calculations

Unlike the p value or rational function form, the optimal F_0 value varies with the molecule and NLO property for which the FF calculation is performed. The strong dependence of the optimal F_0 on the molecule and property can be observed in Figure 2.4. This figure illustrates that F_0 must be picked precisely to minimize error; using an F_0 that is not optimal leads to unusable results. Thus, a method to consistently choose the correct F_0 value is needed. As reference values are not available in practice, only the calculated response property value can be used for choosing F_0. Additionally, the response property cannot be computed for too many F_0 values, since this negates the cost advantage of the FF method.

To develop this method, plots similar to those generated for the least squares analysis (Section 2.3.3) were first used. However, instead of plotting the errors against F_0, the raw values of each computed property were plotted. An example of these plots, where γ is computed for acetamide, is given in Figure 2.5a. It can be observed that deviation from the least squares solution is minimized near the optimal field value, which is represented by the vertical red line. This deviation is quantified by the r value, calculated by Equation (11). Plotting the r value (Figure 2.5b) shows that it reaches a minimum at the optimal field, corresponding to the point at which the curves in Figure 2.5a begin to follow the least squares solution. Thus, starting from the low-field limit and moving toward the high-field limit, the initial field is picked as the field after which the r value consecutively increases or decreases for five F_0 values. The field chosen using these criteria, represented by the purple vertical line in Figure 2.5b, is not exactly at the optimal F_0. This is due to the roughness of r value curve at the minima, which makes it difficult to choose the F_0 value exactly corresponding to the minimum. Overall, this algorithm was used to compute the optimal F_0 for a set of 121 molecules (Figure 5). These F_0 values were used to compute α and γ for each molecule in the 121-molecule set. Similarly, β was computed using the F_0 chosen for a set of 91 non-centrosymmetric molecules (Figure 6). Overall, this field-picking method, along with the optimized common ratio and rational-function model allow for the computation of NLO properties in a quick and reasonably accurate manner.

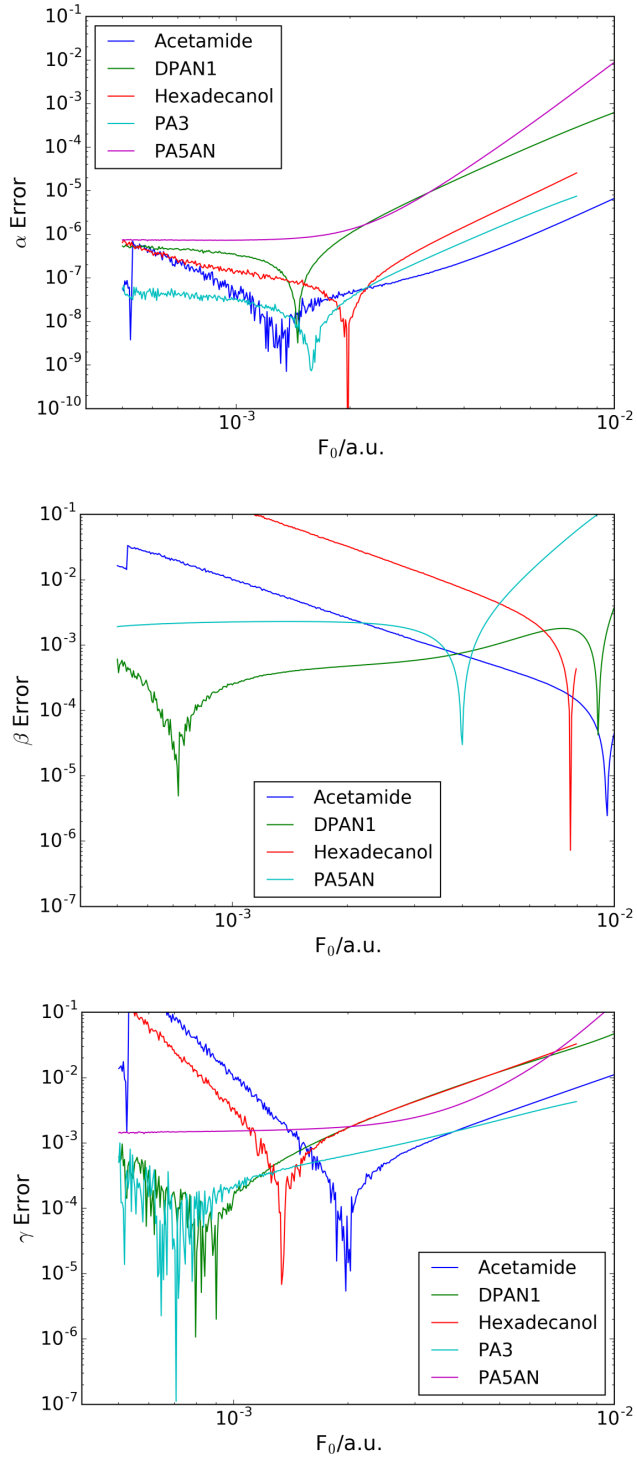

Figure 2.4. The optimal initial field value (F_0) that minimizes the error strongly depends on the molecule and NLO property for which the calculation is run.

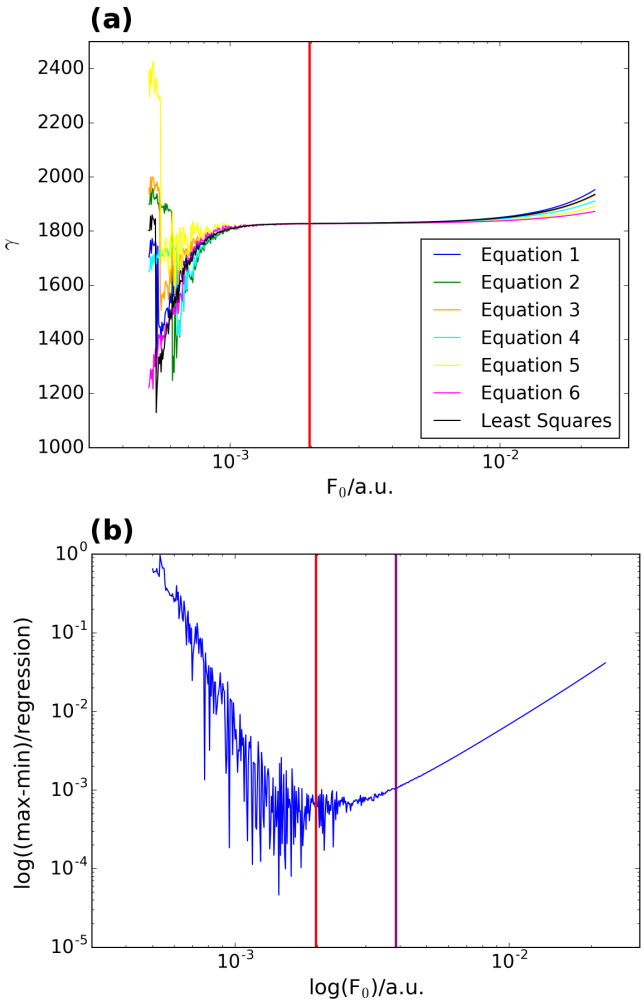

Figure 2.5. Determining a criterion for choosing an optimal initial field for the FF calculation. Both graphs shown are for the computed value of γ for acetamide. The vertical red lines represent the optimal field value. In **(a)**, the deviation of the other solutions from the least squares result decreases as the optimal field value is approached. To determine the deviation from the least squares result, the maximum value of a calculated property can be subtracted from the minimum, and divided by the least squares regression result. A plot of this value is shown in (**b**). As the deviation decreases in plot (a), the curve in plot (b) reaches a minimum. The vertical purple line in plot (b) is the field chosen by the field-picking algorithm.

2.4.5 Comparison of single-molecule error behaviour to the polynomial model

After having optimized the new FF method, its accuracy and behaviour is compared to the previous polynomial model[31]. To start, a single molecule comparison, using acetamide, is done. In general, the trends described for acetamide are representative of those observed for the entire dataset of molecules (Figures 2.6 and 2.7). Errors in α, β, and γ as F_0 is varied were plotted for the rational-function and polynomial models, and are given in Figure 2.8. For the polynomial model, each iterative Richardson extrapolation used to refine the error is denoted as m = 0,1,2,3. For α and γ, the error in the ration-function model is comparable to the m = 2 polynomial refinement. For β, the error in the rational-function model is comparable to m = 1 for the polynomial model. For each property, the error curve for the rational function fit is smoother than the comparable polynomial curve. This smoothness likely reduces the need for error refinement steps. Additionally, the lack of a need for error refinement steps for the rational function model provides advantages in the form of lower computational cost and a simpler implementation.

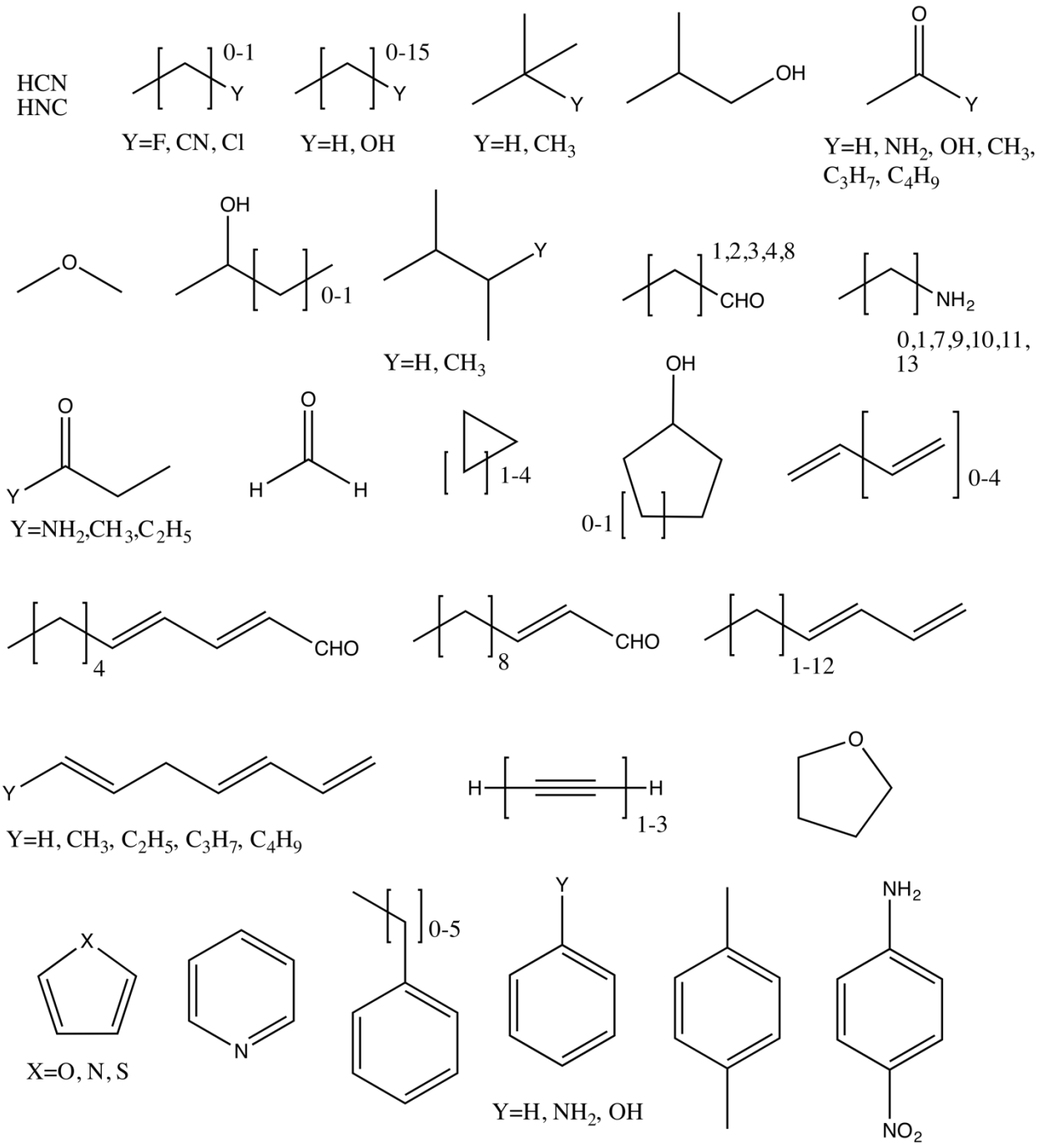

Figure 2.6. The 121 molecules for which α and γ were calculated using the rational-function based FF method.

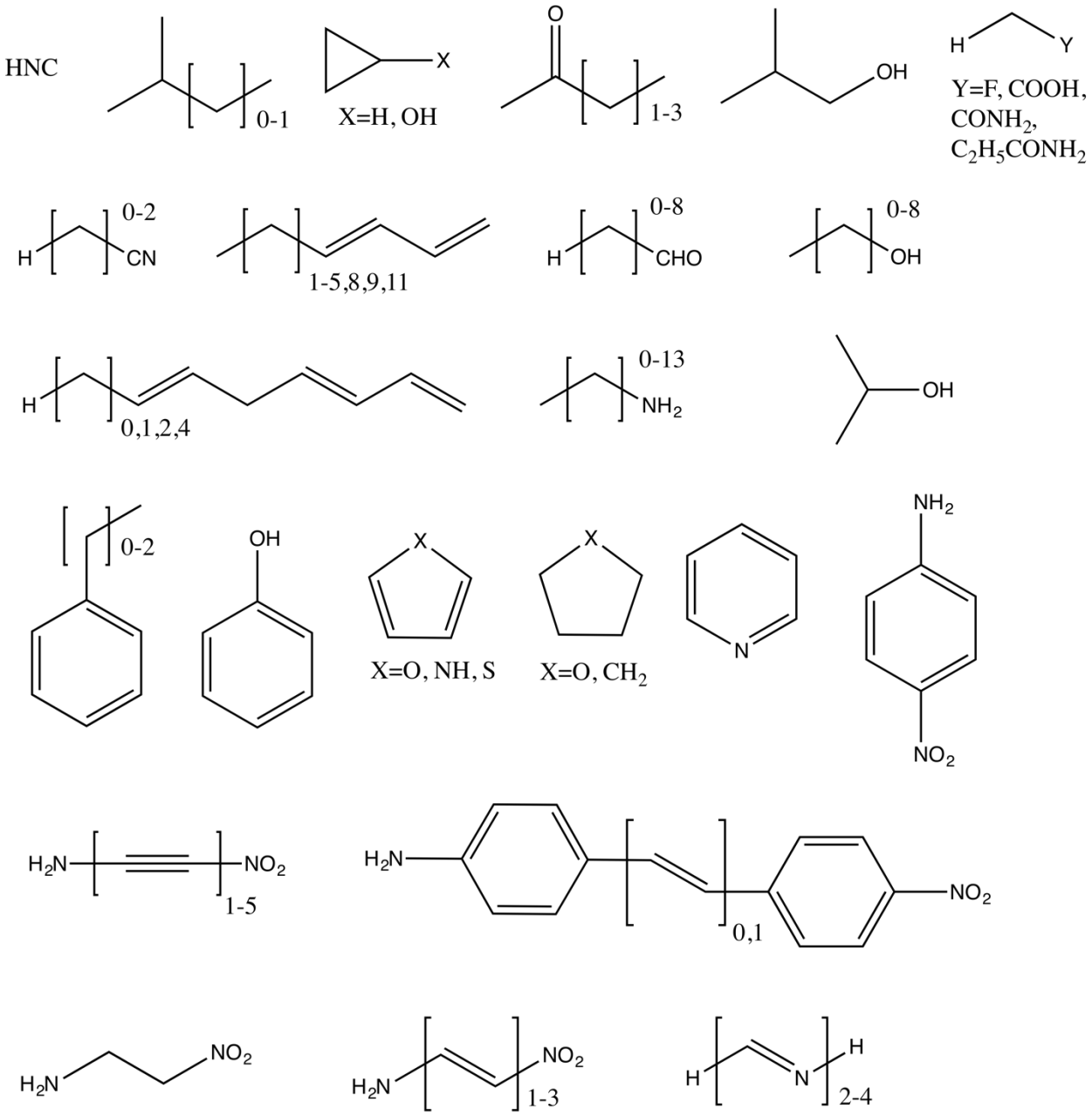

Figure 2.7. The 91 non-centrosymmetric molecules for which β was calculated using the rational-function based FF method.

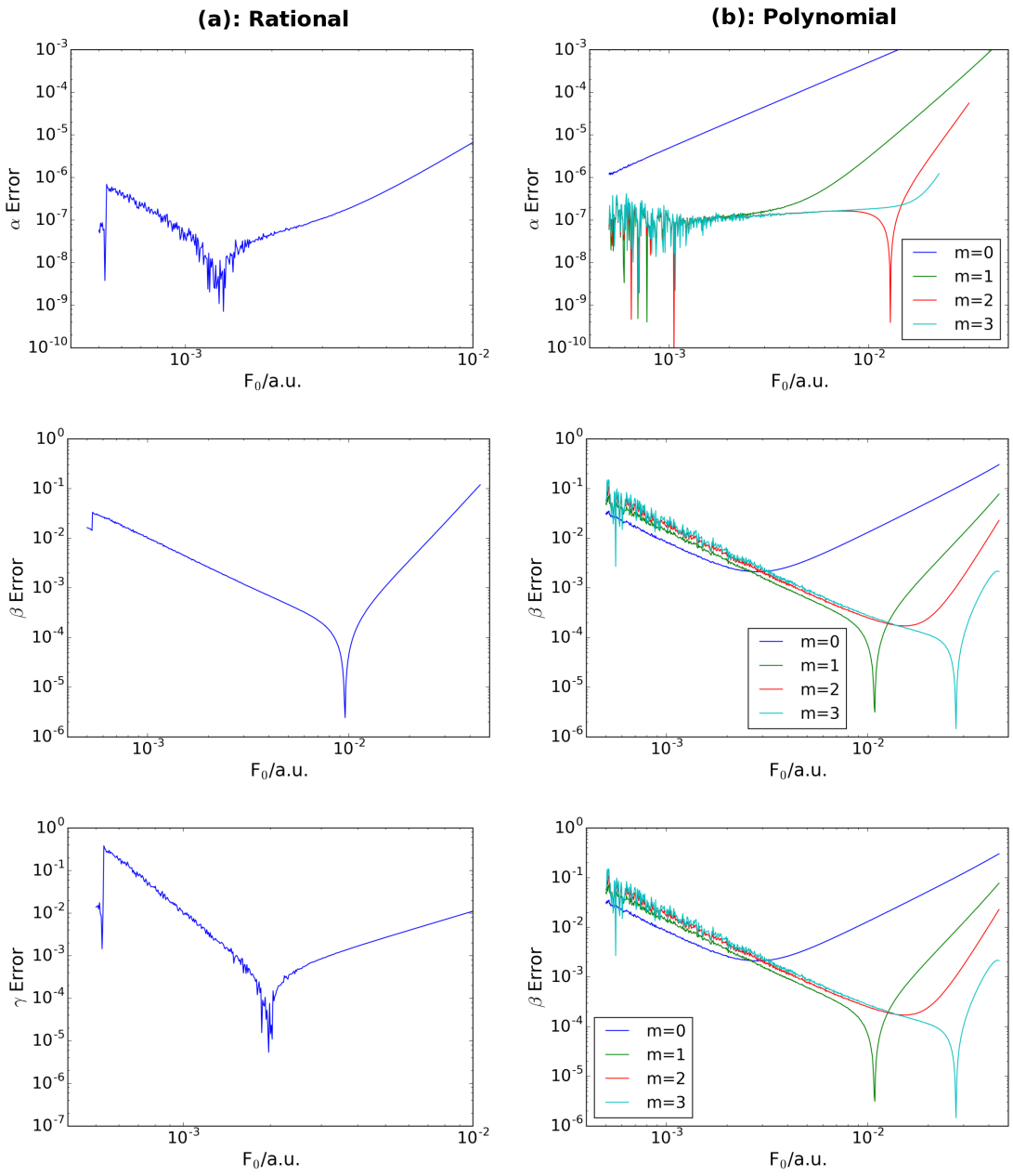

Figure 2.8. The α, β, and γ error behaviour for acetamide is compared between the rational-function (a) and polynomial (b) FF methods. For the polynomial method, the behaviour with iterative refinement via Richardson extrapolation is shown, denoted as *m* = 0,1,2,3.

2.4.6 Overall comparison of the rational-function and polynomial models

To compare the accuracy and robustness of the rational function model versus the polynomial model[31], plots of the average α, β, and γ errors over χ for the entire dataset were created (Figure 2.9). Here, $\chi = \frac{F_0}{F_{0\,(optimized)}}$, where F_0 is the initial field, and $F_{0\,(optimized)}$ is the optimal initial field chosen by the protocol presented in Section 2.4. This normalization allows the average behaviour of the entire dataset to be compared around $F_{0\,(optimized)}$, where χ = 1. Though as many molecules as possible from the dataset were included, the energies of some molecules could not be calculated at enough F_0 values to span the full range of the graph. We found that at the χ values where the data for these molecules ended, large discontinuities in the graph would occur. Thus, these molecules were not included in the graphs. The two major errors in the FF method, truncation and round-off error,[36] can be observed in these graphs. Truncation error increases with increasing F_0 values, and round-off error increases with decreasing F_0 values.

For α, the accuracy at χ = 1 of the rational-function and polynomial models are quite similar, with minimum errors of approximately 10^{-7} for both. However, the rational function model is approximately half an order of magnitude less accurate than the polynomial model. Comparing the behaviour of both models, the rational function model remains at a lower overall error for a large range of fields compared to the polynomial model. This means that the results are robust with respect to moderate errors in choosing the optimal F_0 .

The errors at χ = 1 for β are approximately 10^{-3}, with the rational-function model being half an order of magnitude less accurate than the polynomial model. Similar to α,

the rational function model is more robust to changes in initial field strength. In general, errors are smaller than 10^{-2} for field strengths between χ values of 1-4. This is a greater range than that of the polynomial model, which remains in that range for 0.25-2.5 χ only. Thus, small errors in choosing the optimal F_0 are less detrimental to the accuracy of the rational-function model than the polynomial model.

At $\chi = 1$, the polynomial model[31] obtains average errors on the order of 10^{-4} for γ. The rational function model performs significantly worse, with an accuracy loss of approximately 1.5 orders of magnitude. However, the error for the rational function model remains lower over a larger range of fields, as observed for the α and β calculations. The rational function model consistently remains at an error of 10^{-1} or lower for χ = 0.1-4, in contrast to the polynomial model, which achieves this for χ = 0.1-2.0 only.

Though the comparison above may lead to the conclusion that the rational function model is less accurate overall, this is not the case. Rather, the loss of accuracy is from not having the error minima centered on $\chi = 1$. For α and γ, the minimum error occurs at χ = 0.5, while for β, the minimum error is at $\chi = 2$. This suggests that the protocol used to choose the optimal F_0 value overestimates this value for α and γ, and underestimates it for β. From Figure 4b, it can be observed that the r value becomes smooth only after the minimum is reached. For β, the r value becomes smooth before the minimum is reached. Thus, this over and underestimation of F_0 is expected, as the protocol only chooses the optimal F_0 value when the r value becomes smooth. Though different variations of the protocol were explored, none were able to yield any improvement. Thus, work will be continued on developing a more consistent method to

find the minimum r value. However, despite issues with choosing F_0, the rational function model is more robust with regards to the initial field chosen; overestimation or underestimation of the optimal initial field will still yield reasonably accurate results. The robustness of the rational model is expected, as the rational function reduces the truncation error relative to a polynomial fit, which should increase the range of acceptable field strengths for a calculation. However, the round-off error remains similar for both models, but these errors are controlled by using very tight convergence criteria for the energies, and by selecting the minimum field appropriately. Overall, this robustness to the F_0 value used in the calculation is a key step in improving the overall user-friendliness and reliability of the FF method.

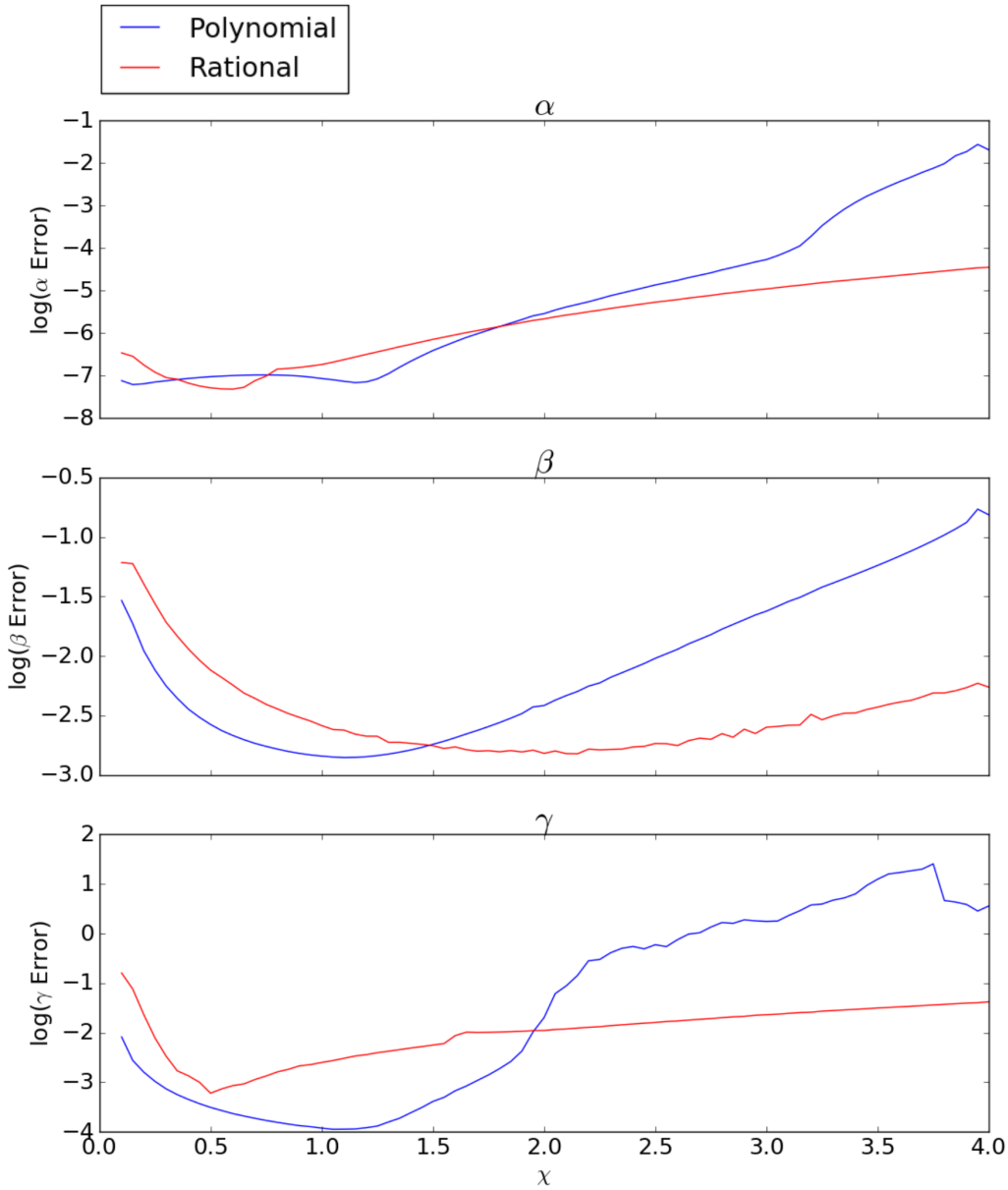

Figure 2.9. The average α, β, and γ error behaviour for the dataset of molecules is compared between the rational-function (red) and polynomial (blue) FF methods. The field values for each molecule are normalized using the optimal initial field value for each molecule. Thus, $\chi = \frac{F_0}{F_{0\,(optimized)}}$, where F_0 is the initial field used for the FF calculation, and $F_{0\,(optimized)}$ is the optimal initial field automatically chosen for the FF calculation. At $\chi = 1$, the overall error for the rational-function model is not as low as for the polynomial model. However, the rational model error remains lower over a larger range of χ, indicating that it is more robust to changes in F_i than the polynomial model. For the polynomial curves (blue), the Richardson refinement level is m = 1 for β, and m= 2 for α and γ.

2.5 Conclusion

A variation of the FF method using a rational function was presented to calculate longitudinal polarizability and the first and second longitudinal hyperpolarizabilities of a wide range of molecules. To calculate NLO properties accurately, the functional form to best fit the energy was found, along with the optimal field distribution and a method of choosing F_0 reasonably well. The fitted rational function approximation has a polynomial of degree three in the numerator and a polynomial of degree two in the denominator. The field mesh used for this approximant was generated using a geometric progression with a common ratio of $\sqrt{2}$. To generate a good F_0 guess, it was found that the deviation from the least squares result could be used.

Comparison of the optimized rational-function FF method to the polynomial FF method from ref. 31 shows that both perform similarly with regards to error behaviour. Unlike the polynomial model, the rational function model does not need subsequent error refinement. This is advantageous in terms of computational cost, and for ease of implementation. Comparison of the two methods for the overall dataset reveals that the rational-function FF method loses approximately 0.5-1.5 orders of magnitude in accuracy relative to the polynomial method. However, the insensitivity of the rational-function FF method to F_0, along with not requiring refinement steps, makes this method a strong choice for new quantum chemistry codes that wish to implement a cheap and simple method for NLO property calculations.

2.6 Bibliography

(1) Franken, P. A.; Hill, A. E.; Peters, C. W.; Weinreich, G. Generation of Optical

Harmonics. *Phys. Rev. Lett.* **1961**, *7*, 118–119.

(2) Nalwa, H. S.; Miyata, S. *Nonlinear Optics of Organic Molecules and Polymers*; CRC Press, 1997.

(3) Brédas, J. L.; Adant, C.; Tackx, P.; Persoons, A.; Pierce, B. M. Third-Order Nonlinear Optical Response in Organic Materials: Theoretical and Experimental Aspects. *Chem Rev* **1994**, *94*, 243–278.

(4) Luo, Y.; Ågren, H.; Jørgensen, P.; Mikkelsen, K. V. Response Theory and Calculations of Molecular Hyperpolarizabilities. *Adv. Quantum Chem.* **1995**, *26*, 165–237.

(5) Prasad, P. N.; Williams, D. J. *Introduction to Nonlinear Optical Effects in Molecules and Polymers*; Wiley, 1991.

(6) Caves, T. C.; Karplus, M. Perturbed Hartree–Fock Theory. I. Diagrammatic Double-Perturbation Analysis. *J. Chem. Phys.* **1969**, *50*, 3649–3661.

(7) Gerratt, J.; Mills, I. M. Force Constants and Dipole-Moment Derivatives of Molecules from Perturbed Hartree–Fock Calculations. II. Applications to Limited Basis-Set SCF–MO Wavefunctions. *J. Chem. Phys.* **1968**, *49*, 1730–1739.

(8) Stevens, R. M.; Pitzer, R. M.; Lipscomb, W. N. Perturbed Hartree—Fock Calculations. I. Magnetic Susceptibility and Shielding in the LiH Molecule. *J. Chem. Phys.* **1963**, *38*, 550–560.

(9) Jansik, B.; Sałek, P.; Jonsson, D.; Vahtras, O.; Ågren, H. Cubic Response Functions in Time-Dependent Density Functional Theory. *J. Chem. Phys.* **2005**, *122*, 54107.

(10) Helgaker, T.; Coriani, S.; Jørgensen, P.; Kristensen, K.; Olsen, J.; Ruud, K. Recent Advances in Wave Function-Based Methods of Molecular-Property Calculations. *Chem. Rev.* **2012**, *112*, 543–631.

(11) Cohen, H. D.; Roothaan, C. C. J. Electric Dipole Polarizability of Atoms by the Hartree—Fock Method. I. Theory for Closed-Shell Systems. *J. Chem. Phys.* **1965**, *43*, S34–S39.

(12) Maroulis, G.; Bishop, D. M. On the Dipole and Higher Polarizabilities of Ne(1S). *Chem. Phys. Lett.* **1985**, *114*, 182–186.

(13) Maroulis, G.; Thakkar, A. J. Multipole Moments, Polarizabilities, and Hyperpolarizabilities for N_2 from Fourth-order Many-body Perturbation Theory Calculations. *J. Chem. Phys.* **1988**, *88*, 7623–7632.

(14) Bishop, D. M.; Pipin, J.; Lam, B. Field and Field-Gradient Polarizabilities of BeH, BH and CH^+. *Chem. Phys. Lett.* **1986**, *127*, 377–380.

(15) Bishop, D. M.; Pipin, J. Field and Field-Gradient Polarizabilities of H_2O. *Theor. Chim. Acta* **1987**, *71*, 247–253.

(16) Kurtz, H. A.; Stewart, J. J. P.; Dieter, K. M. Calculation of the Nonlinear Optical Properties of Molecules. *J. Comput. Chem.* **1990**, *11*, 82–87.

(17) Bartlett, R. J.; Purvis, G. D. Molecular Hyperpolarizabilities. I. Theoretical Calculations Including Correlation. *Phys. Rev. A* **1979**, *20*, 1313–1322.

(18) Bulat, F. A.; Toro-Labbé, A.; Champagne, B.; Kirtman, B.; Yang, W. Density-Functional Theory (Hyper)polarizabilities of Push-Pull π-Conjugated Systems: Treatment of Exact Exchange and Role of Correlation. *J. Chem. Phys.* **2005**, *123*, 14319.

(19) Wouters, S.; Limacher, P. A.; Van Neck, D.; Ayers, P. W. Longitudinal Static Optical Properties of Hydrogen Chains: Finite Field Extrapolations of Matrix Product State Calculations. *J. Chem. Phys.* **2012**, *136*, 134110.

(20) Nénon, S.; Champagne, B.; Spassova, M. I. Assessing Long-Range Corrected Functionals with Physically-Adjusted Range-Separated Parameters for Calculating the Polarizability and the Second Hyperpolarizability of Polydiacetylene and Polybutatriene Chains. *Phys. Chem. Chem. Phys.* **2014**, *16*, 7083.

(21) Matsui, H.; Nakano, M.; Champagne, B. Theoretical Study on the Spin State and Open-Shell Character Dependences of the Second Hyperpolarizability in Hydrogen Chain Models. *Phys. Rev. A* **2016**, *94*, 42515.

(22) de Wergifosse, M.; Liégeois, V.; Champagne, B. Evaluation of the Molecular Static and Dynamic First Hyperpolarizabilities. *Int. J. Quantum Chem.* **2014**, *114*, 900–910.

(23) Medved', M.; Jacquemin, D. Tuning the NLO Properties of Polymethineimine Chains by Chemical Substitution. *Chem. Phys.* **2013**, *415*, 196–206.

(24) Sekino, H.; Maeda, Y.; Kamiya, M.; Hirao, K. Polarizability and Second Hyperpolarizability Evaluation of Long Molecules by the Density Functional Theory with Long-Range Correction. *J. Chem. Phys.* **2007**, *126*, 14107.

(25) Salustro, S.; Maschio, L.; Kirtman, B.; Rérat, M.; Dovesi, R. Third-Order Electric Field Response of Infinite Linear Chains Composed of Phenalenyl Radicals. *J. Phys. Chem. C* **2016**, *120*, 6756–6761.

(26) Jacquemin, D.; Perpète, E. A.; Medved', M.; Scalmani, G.; Frisch, M. J.;

Kobayashi, R.; Adamo, C. First Hyperpolarizability of Polymethineimine with Long-Range Corrected Functionals. *J. Chem. Phys.* **2007**, *126*, 191108.

(27) de Wergifosse, M.; Wautelet, F.; Champagne, B.; Kishi, R.; Fukuda, K.; Matsui, H.; Nakano, M. Challenging Compounds for Calculating Hyperpolarizabilities: *P* -Quinodimethane Derivatives. *J. Phys. Chem. A* **2013**, *117*, 4709–4715.

(28) de Wergifosse, M. Approximate Spin-Projected Density-Based Romberg Differentiation Procedure to Evaluate the Second-Hyperpolarizability of *P* -Quinodimethane and Twisted Ethylene and Their Diradical Character Dependence. *J. Phys. Chem. A* **2016**, *120*, 2727–2736.

(29) Wouters, S.; Van Speybroeck, V.; Van Neck, D. DMRG-CASPT2 Study of the Longitudinal Static Second Hyperpolarizability of All-Trans Polyenes. *J. Chem. Phys.* **2016**, *145*, 54120.

(30) Bishop, D. M.; Solunac, S. A. Breakdown of the Born-Oppenheimer Approximation in the Calculation of Electric Hyperpolarizabilities. *Phys. Rev. Lett.* **1985**, *55*, 1986–1988.

(31) Mohammed, A. A. K.; Limacher, P. A.; Champagne, B. Finding Optimal Finite Field Strengths Allowing for a Maximum of Precision in the Calculation of Polarizabilities and Hyperpolarizabilities. *J. Comput. Chem.* **2013**, *34*, 1497–1507.

(32) Aidas, K.; Angeli, C.; Bak, K. L.; Bakken, V.; Bast, R.; Boman, L.; Christiansen, O.; Cimiraglia, R.; Coriani, S.; Dahle, P.; et al. The Dalton Quantum Chemistry Program System. *Wiley Interdiscip. Rev. Comput. Mol. Sci.* **2014**, *4*, 269–284.

(33) Rassolov, V. A.; Ratner, M. A.; Pople, J. A.; Redfern, P. C.; Curtiss, L. A. 6-31G* Basis Set for Third-Row Atoms. *J. Comput. Chem.* **2001**, *22*, 976–984.

(34) Champagne, B.; Perpète, E. a; Jacquemin, D.; van Gisbergen, S. J. a; Baerends, E. J.; Soubra-Ghaoui, C.; Robins, K. a; Kirtman, B. Assessment of Conventional Density Functional Schemes for Computing the Dipole Moment and (Hyper)polarizabilities of Push-Pull π-Conjugated Systems. *J. Phys. Chem. A* **2000**, *104*, 4755–4763.

(35) Limacher, P. A.; Li, Q.; Lüthi, H. P. On the Effect of Electron Correlation on the Static Second Hyperpolarizability of π Conjugated Oligomer Chains. *J. Chem. Phys.* **2011**, *135*, 14111.

(36) Ruden, T. A.; Taylor, P. R.; Helgaker, T. Automated Calculation of Fundamental Frequencies: Application to AlH_3 Using the Coupled-Cluster Singles-and-Doubles with Pertubative Triples Method. *J. Chem. Phys.* **2003**, *119*, 1951–1960.

Chapter 3

Resummation of the Møller-Plesset Perturbation Series using Gauss Hypergeometric Functions

3.1 Motivation

Within computational chemistry, one of the major goals is to be able to compute the energies of molecules and materials. This allows for the simulation of many different properties, and is particularly foundational to the computation of nonlinear optical (NLO) properties using the finite field[1–5] method. Though computing NLO properties using the finite field method is quick, the computation of molecular energies represents a rate-

limiting step in the overall process, as these calculations can take up to months to complete.

The issue with computing the energy for a system is the tradeoff between accuracy, and the overall computational cost of the calculation.[6] The larger the system, the more computational cost associated with determining the energy. Consequently, one must resort to computationally cheap methods to be able to solve for the energy of larger systems, but this may not be accurate. Thus, in this study, we set out to determine a means of taking relatively cheap computations, and refining them systematically to increase accuracy, with minimal added computational time. This allows many larger systems, especially those of biological relevance, to be investigated with greater ease.

3.2 Introduction

The field of computational chemistry aims to accurately simulate and predict chemical phenomena. This includes both simulation of molecules, reactions and materials. Though there are many problems within the scope of computational chemistry, the computation of energy remains a fundamental calculation that forms a foundation to be able to answer many questions posed by computational chemists. The critical nature of computing accurate molecular energies has lead to a plethora of different methods, each with their own unique strengths and drawbacks.

Within quantum chemistry, we can fundamentally categorize all *ab initio* energy calculation methods as being either Electronic Structure Theory (EST) based, or Density Functional Theory (DFT) based.[6] EST is based off of solving the time independent Schrodinger Equation:

$$\hat{H}\Psi(R_1, R_2 \dots R_N, r_1, r_2 \dots r_N) = E\Psi(R_1, R_2 \dots R_N, r_1, r_2 \dots r_N) \quad \text{Eq. 3.1}$$

However, as this equation is not exactly solvable for systems with more than one electron, those developing EST methods must make a series of assumptions to render this equation tractable. In general, one of the key advantages to using, and developing, EST methods is the ability to systematically improve the method, as we exactly know the correct form that needs to be solved. However, though there are EST methods that are quite computationally cheap, using accurate EST methods tends to be quite expensive. This is not necessarily the case with DFT-based methods.

DFT based methods are based off of the Hohenburg-Kohn theorem[7], which postulate that the electronic energy of a molecule can be written as a functional of the electron density. This greatly simplifies the computation of molecular energy, from a problem that handles N-electrons with 3N coordinates, to a problem that only relies on only three coordinates. Later work by Kohn-Sham[8] led to the following equation to express molecular energy as a functional of electron density:

$$E[\rho] = T_s[\rho] + E_{ne}[\rho] + J[\rho] + E_{xc}[\rho] \qquad \text{Eq. 3.2}$$

Where the total energy ($E[\rho]$) is expressed as a sum of the kinetic energy ($T_s[\rho]$), nuclear-electron attraction ($E_{ne}[\rho]$), Coloumb repulsion between electrons ($J[\rho]$), and the exchange-correlation energy ($E_{xc}[\rho]$).

Of these four terms, computing the first three are relatively straightforward. However, the exchange correlation energy is quite tricky to determine, with no way of knowing the exact form that it takes. Determining good approximations for this term tends to be a challenge for those developing DFT based methods. Not knowing the exact form that this term takes also represents one of the greatest drawbacks for DFT based methods, which is that one cannot improve the accuracy of results in a systematic fashion

similar to EST methods. However, DFT based methods tend to be cheaper, while providing comparable accuracy to EST methods. This inexpensiveness is why DFT based methods are widely relied upon by computational chemists.

In this study, we chose to develop a perturbation series[9] based method. These methods fall into the category of being EST based, and start with an uncorrected energy. Then, corrections are added to this energy in the form of higher order terms in the series. To determine more accurate energies, one simply computes as many terms as desired. The number of terms that can be computed is limited only by system size, computational power available, and time available to run the calculation.

One of the most widely used perturbation series in computational chemistry is the Møller-Plesset (MP) perturbation series[10]. This series starts with the sum of occupied orbital energies, which does not include any electron correlation. Subsequent terms in the series add more electron correlation effects, which (in principle) increase the accuracy of the energy computed. However, this series is well known to be divergent for many systems in the infinite limit.[11] Thus, a resummation method must be used to produce a convergent series from this divergent one. In this study, we chose to use hypergeometric resummation[12] as a tool to be able to extrapolate the MP series to the infinite limit.

We chose this resummation approach[12] for several reasons. The first is that the calculation of MP1-4 energies is relatively cheap, and can easily be done for many systems of biological relevance. This is important to the more widespread adoption of computational chemistry tools in the fields of biochemistry and chemical biology. There are also many MP1-4 energies reported in the literature, which allows many systems to be studied with greater accuracy, but without having to run further calculations.

Additionally, the hypergeometric resummation approach provides a lightweight tool that does not add (virtually) any computational cost to the MP4 calculation. Finally, this approach leaves many options for systematic improvement; one can use more general functions in an attempt to obtain a more accurate resummation. This preserves one of the advantages of EST based methods.

The hypergeometric function we are using to fit the energies is the Gauss hypergeometric function. This function has the following form:

$$ {}_kF_l\left(\begin{matrix}a_1,\dots,a_k\\ b_1,\dots,b_l\end{matrix}\middle| c\right) = \sum_{n=0}^{\infty}\frac{(a_1)_n\dots(a_k)_n}{(b_1)_n\dots(b_l)_n}(cx)^n \qquad \text{Eq. 3.3} $$

Where $(a)_n$ are Pochhammer symbols, written in terms of gamma functions:

$$ (a)_n = \frac{\Gamma(a+n)}{\Gamma(a)} \qquad \text{Eq. 3.4} $$

From Equation 3.4 it can be observed that the structure of this function is combanatoric; this allows for a high degree of flexibility when fitting.

Overall, we will be using the Gauss hypergeometric function to fit the energies obtained from MP1-4 calculations. Then, the resummed hypergeometric function will be used to extrapolate to the infinite limit of the MP series, which should provide us with a computationally cheap means of refining the energy obtained from MP1-4 calculations. To test this method, we will be using strongly correlated systems (Methods 3.3.2), as they are quite small, so we can compute reference energies using full CI. Additionally, these systems are quite difficult to compute accurately for most computational methods, so they represent a rigorous test for this newly developed protocol.

3.3 Methods

3.3.1 Overview of the Resummation Scheme

In most perturbation series[9], we have a perturbation parameter (ε) that is dimensionless, and which is quite small in magnitude, ε << 1. We can expand the energy of a molecule using a Taylor series, written in terms of this parameter, and centered around *a*:

$$E(a+\varepsilon) = E(a) + \varepsilon E'(a) + \frac{1}{2!}\varepsilon^2 E''(a) + \frac{1}{3!}\varepsilon^3 E'''(a) + \frac{1}{4!}\varepsilon^4 E^{(4)}(a) + \cdots \quad \text{Eq. 3.5}$$

If we choose $a = 0$, and substitute $\varepsilon = 1$ into this series, then we obtain the following expression:

$$E(1) = E(0) + E'(0) + \frac{1}{2!}E''(0) + \frac{1}{3!}E'''(0) + \frac{1}{4!}E^{(4)}(0) + \cdots \quad \text{Eq. 3.6}$$

We can think of the perturbation parameter, ε as a means of measuring the amount of electron correlation that is considered, where $\varepsilon = 0$ gives us a simple sum of occupied orbitals, and $\varepsilon = 1$ is the "true" corrected molecular energy. Thus, the expression in Equation 3.6 would give us the true energy, if we were able to solve this series analytically. What becomes interesting, is that the derivatives in this expression can be thought of as subsequent corrections to the uncorrelated (E(0) energy as follows:

$$\begin{gathered} E(0) = \sum_{i \in occ} \varepsilon_i \\ E'(0) = E_{HF} - E(0) \\ E''(0) = E_{MP2} - E_{HF} \\ E^{(n)} = n!\,(E_{MPn} - E_{MPn-1}) \end{gathered} \quad \text{Eq. 3.7}$$

Where E(0) represents the sum of all occupied alpha orbital energies, HF is the Hartree-Fock Energy (equivalent to MP1), and MPn is the nth-order MP energy. Most standard quantum chemistry software can compute up to the MP4 energy. In this study, we used Gaussian 09, Rev. C.01[13] to compute the occupied alpha orbital, and MP1-4 energies. The basis set for these calculations was minimal (STO-3G[14,15]). All calculations were

checked for normal termination, and convergence. This gives us up to 5 terms in the series (Equation 3.6).

Once we have the numbers for each of the terms, we move to creating a system of equations with our hypergeometric function, of the form $_2F_1$ (Equation 3.3). To do so, we first divide our series by E(0) to normalize the first term to 1. Next, we define $O_n = \delta o_n U^n$, where n represents the n-th term, and we can rewrite our series in the following way:

$$E(1) \approx 1 + \delta o_1 U + \frac{1}{2!}\delta o_2 U^2 + \frac{1}{3!}\delta o_3 U^3 + \frac{1}{4!}\delta o_4 U^4 \qquad \text{Eq. 3.8}$$

Finally, we set the third parameter in the hypergeometric function (Equation 3.3) to $c = cU$. Finally, each of the respective four terms can be equated to form a system of nonlinear equations, as follows:

$$\delta o_n = \frac{(a_1)_n (a_2)_n \ldots}{(b_1)_n}(cx)^n \qquad \text{Eq. 3.9}$$

Where n ranges from 1-4. This system of equations was then solved using the Python scipy.optimize package, using the lst_squares nonlinear equation solver. Care was taken to ensure that the optimality of the optimized function was less than 10^{-9}, ensuring tight convergence. If this optimality was not reached, another random initial guess was chosen, and the function was re-optimized until converged sufficiently.

Once the optimized function parameters for the function were determined, the hypergeometric series was solved with these parameters at x = 1. This solved energy should be a close approximation to the case when ε = 1, giving an energy that is closer to the "true" correlated energy.

3.3.2 Overview of Test Systems

The test systems that were used in this study were mostly those that are known to display strong correlation behavior. This includes hydrogen atom chains (H_2 and H_4), and several diatomics (N_2, O_2^{2+}, C_2). The diatomic molecules were tested at the ground state, and at one or two excited states. The bond lengths in the molecule were stretched from 1.0-10.0 Å, in increments of 0.5 Å.

To provide a reference for the computed energies, Full CI calculations were used. These calculations were done using Gaussian 09, Rev. C.01[13] using the CASSCF keyword, and using all the electrons as part of the active space. The basis set for these calculations was minimal (STO-3G[14,15]). All calculations were checked for normal termination, and proper convergence.

3.4 Results and Discussion

3.4.1 Method Convergence Issues

As this method involves optimizing a system of nonlinear equations (Equation 3.9), it is important that the method is able to converge consistently to determine a correct set of parameters. This is also important for user-friendliness and reliability of the method. If the method fails to converge, then users might need to troubleshoot. If the method does converge, but to the incorrect minima, then the results from the method cannot be trusted.

As expected in this study, we found that the nonlinear solver tended to have issues with convergence. Sometimes the nonlinear solver would converge to local minima, rather than the global minima. This would lead to an ill-fitted function, which then would

provide drastically incorrect energies when used to extrapolate the MP series. However, observing the fitted function optimality, which is a measure of how close the fitted function is to the original points, allows one to know if the function was optimized to a local minima. It was determined though observation that if the optimality was above 10^{-9}, then the function was not converged properly. Having this measure greatly increases the reliability of the method, as the optimization can be set to rerun with another random guess if a local minima is found.

In order to assess if changing convergence tolerances would help with finding global minima instead of local ones, the same calculations were rerun several times with increasing and decreasing tolerances. The three tolerances parameters in the solver, called xtol, gtol and ftol were independently set from 10^{-6} to 10^{-13}, decreasing an order of magnitude each trial. It was found that decreasing the default tolerance of 10^{-9} for any of these parameters did not help find global maxima more easily.

Although several different nonlinear solvers as part of the scipy.optimize package were tried, none were found to work substantially better than the lst_squares optimizer. The other optimizers also tended to be much more complex, making output much harder to read; this makes it more difficult to tell when the function had failed to optimize properly. Thus, we decided to continue the remainder of the study with the lst_squares optimizer.

3.4.2 Energy Refinement Results

The reference (FCI), MP4 and refined hypergeometric energies were plotted for each of the test systems (Figures 3.1-3.9). The refined hypergometric energies for these systems displays several general trends and patterns of behaviour. Observing the plots for

the H_2 and H_4 test systems (Figures 3.1 and 3.2), one can observe that the hyergeometric function tends to diverge much more rapidly than the curve for the MP4 series as the bond is stretched. This seems to be a trend that is exclusive to the hydrogen-based test systems, which would have intuitively been thought of as the simplest systems to predict properties of, due to having fewer electrons.

However, despite the high levels of divergence, the hypergeometric function succeeds in refining the energies of the hydrogen-chain systems at lower bond lengths. Often, the accuracy of the MP4 calculation is increased from within 10 millihartrees of the reference value to within 1 millihartree of the FCI value. This leads to the notion that, for strongly correlated hydrogen-based systems, the MP series displays quite erratic behaviour, surpassing the ability of even the general hypergeometric function to be able to accurately resum the data involved. However, at lower bond lengths, the resummation scheme works as intended.

For the remainder of the diatomic systems (Figures 3.3-3.9), the overall trend seems to be more encouraging. For these systems, the hypergeometric function seems to be refining the energy, as predicted. Additionally, many of the large deviations of the MP4 energy from the FCI energy seem to have been minimized, suggesting that fitting using the hypergeometric function does resum the divergent MP series to produce a convergent series with corrected behaviour.

However, these positive results have minor issues that can be observed. Occasionally, we observe that at higher bond lengths, we get results that diverge quite suddenly. Two examples of this is the refined energy for spin 1 N_2, at a bond length of 8.5 Å (Figure 3.3), and the spin 1 O_2^{2+} energy, at a bond length of 7.5 Å (Figure 3.5).

Interestingly, these types of divergences are only observed for the spin 1 diatomic molecules, which have the same electron configuration. It is quite possible that there are issues with refining the MP series for this electron configuration, but further studies need to be conducted. In particular, it would be interesting to determine the hypergeometric refinement curves for C_2^{2-}, to see if a similar trend is observed to that of O_2^{2+} and N_2. If a similar trend were found, this would point to errors that arise from the fit of the MP series, rather than being an artifact of the optimization process.

It would also be interesting to study why the hydrogen chain systems are quite difficult to refine. To do so, there are several possible routes, including testing isoelectronic systems, such as He^+ chains, or to use alternative fitting functions to determine if there is an issue with the form of the hypergeometric function used. It is also possible that more terms in the hypergeometric function are needed, perhaps using a ${}_2F_2$ or ${}_3F_2$ form. To do so, however, MP5 and MP6 energies would be needed, which are generally quite difficult to obtain from commercial quantum chemistry software.

Finally, there are some molecules that do not have refined hypergeometric numbers at higher bond lengths, but also do not show high levels of divergence. These bond lengths are those that the function could not be optimized for, suggesting that there were either no global minima that could be found at those points, or that the nonlinear solver was not robust enough to determine the roots of the system. In future work, it would be interesting to use schemes that provide explicit formulae to optimize the hypergeometric fitting function, to narrow down if the issue is with the nonlinear solver, or the function itself. One resummation scheme that shows promise is based off of Meijer-G functions.[16]

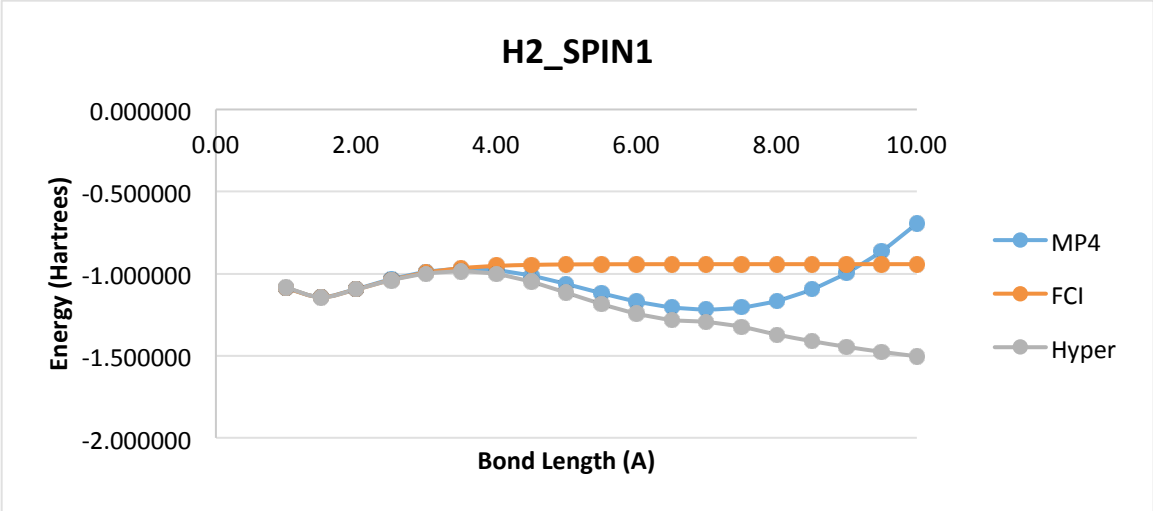

Figure 3.1 Comparison of the MP4, reference (FCI) and hypergeometric energies for H_2 with a spin multiplicity of 1.

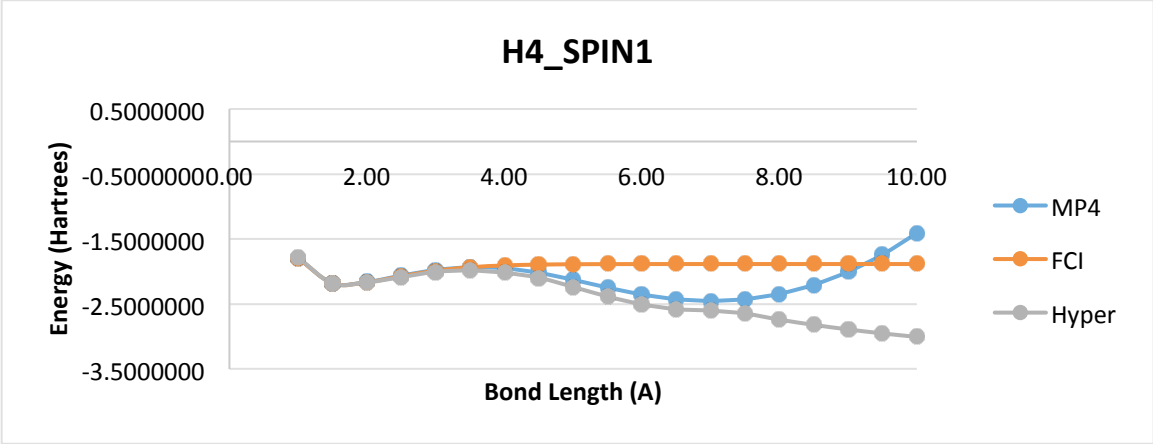

Figure 3.2 Comparison of the MP4, reference (FCI) and hypergeometric energies for H_4 with a spin multiplicity of 1.

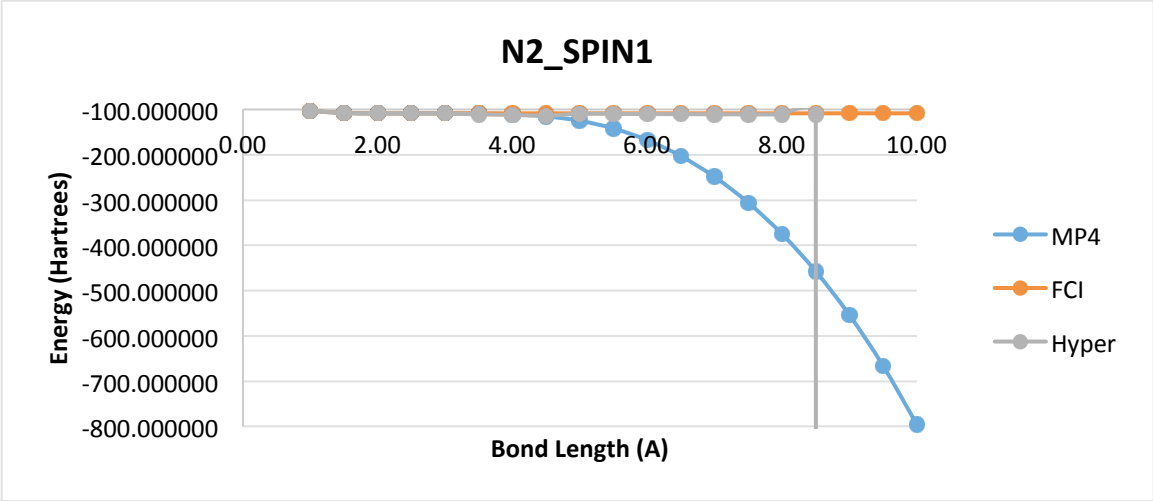

Figure 3.3 Comparison of the MP4, reference (FCI) and hypergeometric energies for N_2 with a spin multiplicity of 1.

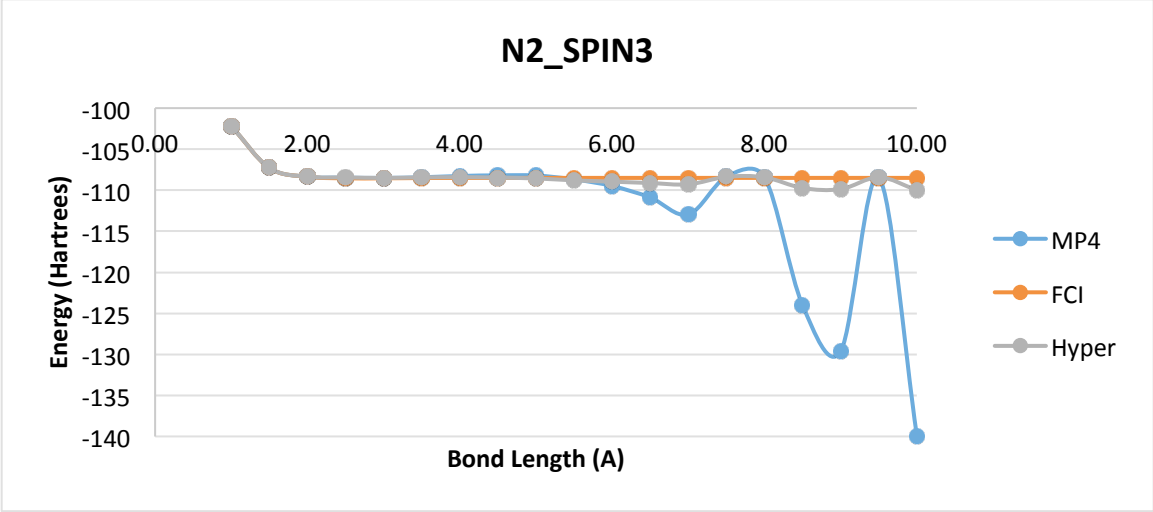

Figure 3.4 Comparison of the MP4, reference (FCI) and hypergeometric energies for N_2 with a spin multiplicity of 3.

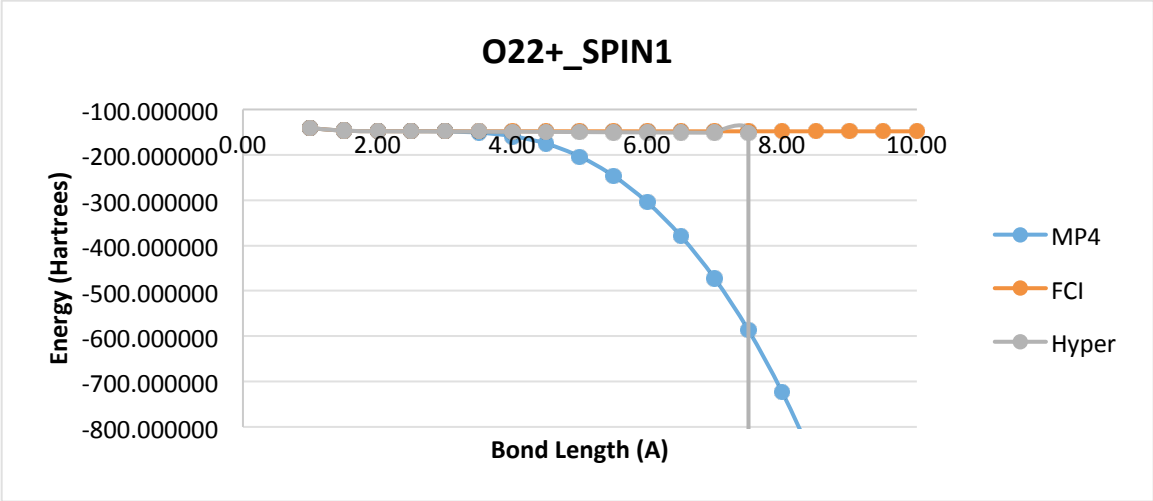

Figure 3.5 Comparison of the MP4, reference (FCI) and hypergeometric energies for O_2^{2+} with a spin multiplicity of 1.

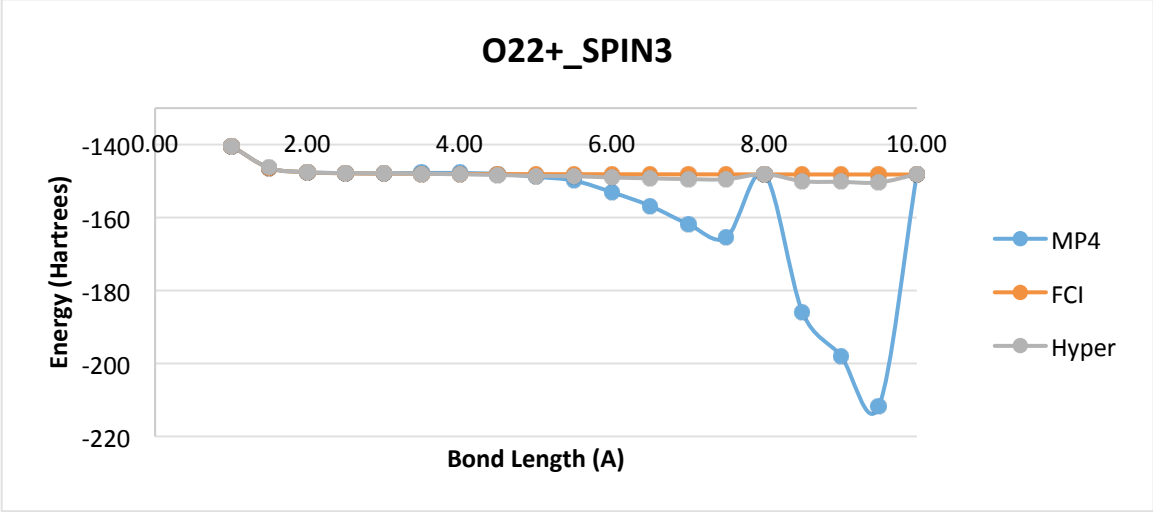

Figure 3.6 Comparison of the MP4, reference (FCI) and hypergeometric energies for O_2^{2+} with a spin multiplicity of 3.

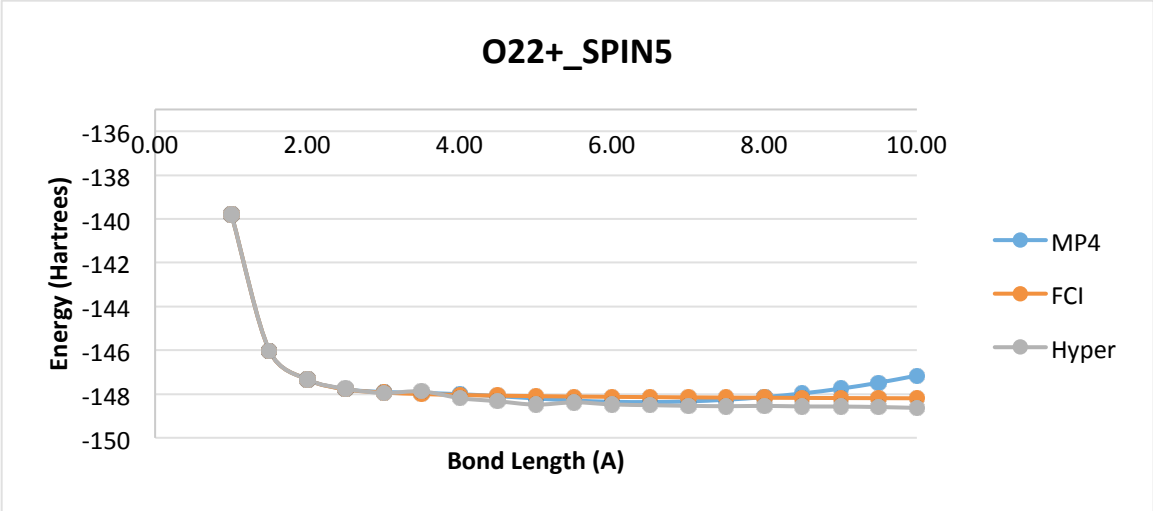

Figure 3.7 Comparison of the MP4, reference (FCI) and hypergeometric energies for O_2^{2+} with a spin multiplicity of 5.

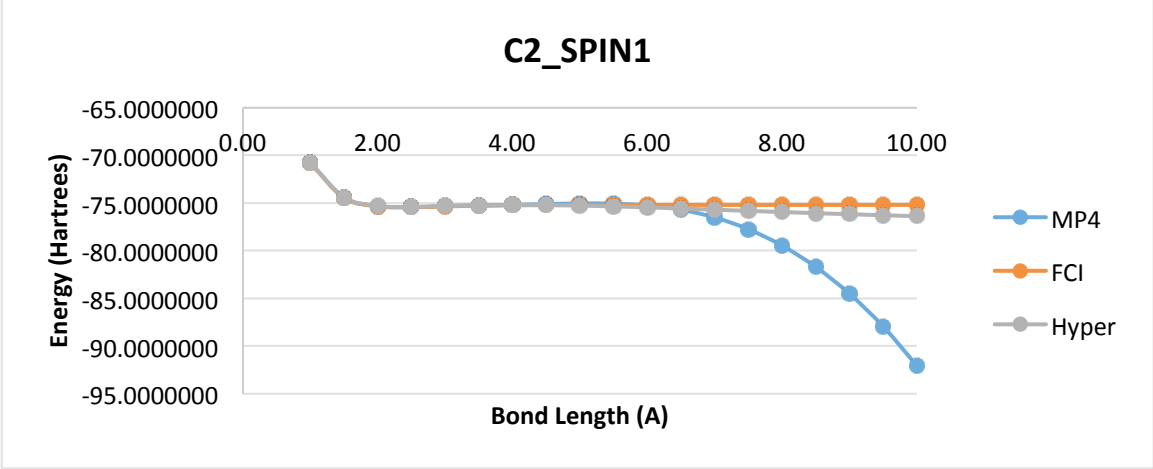

Figure 3.8 Comparison of the MP4, reference (FCI) and hypergeometric energies for C_2 with a spin multiplicity of 1.

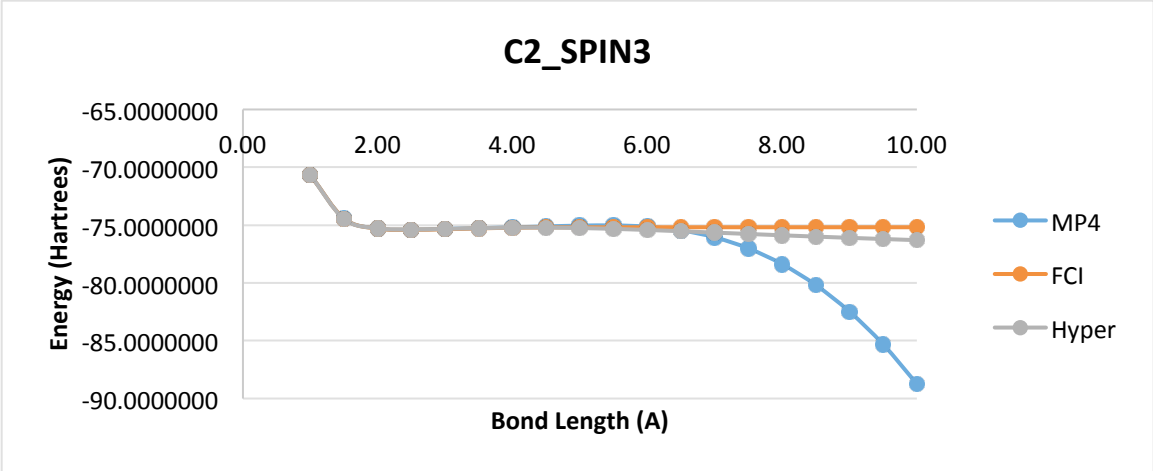

Figure 3.9 Comparison of the MP4, reference (FCI) and hypergeometric energies for C_2 with a spin multiplicity of 3.

3.5 Conclusions and Future Work

Overall, this study shows that the hypergeometric function is a viable method to resum the MP perturbation series for several cases. It was found that for non-hydrogen systems, hypergeometric resummation helped refine the energies, and often helped recover the correct trend for the energy as bonds were dissociated. However, there are issues with the reliable optimization of these functions, which may be solved through using more explicit equations to determine the optimized equations. Additionally, some work still remains on understanding why the function fails to optimize for hydrogen-based test systems, and for particular electron configurations. Finally, the energy refinement needs to be tested for larger systems, including different organic molecules, and systems relevant to biological applications.

3.6 References

(1) Cohen, H. D.; Roothaan, C. C. J. Electric Dipole Polarizability of Atoms by the Hartree—Fock Method. I. Theory for Closed-Shell Systems. *J. Chem. Phys.* **1965**, *43*, S34–S39.

(2) Maroulis, G.; Bishop, D. M. On the Dipole and Higher Polarizabilities of Ne(1S). *Chem. Phys. Lett.* **1985**, *114*, 182–186.

(3) Maroulis, G.; Thakkar, A. J. Multipole Moments, Polarizabilities, and Hyperpolarizabilities for N_2 from Fourth-order Many-body Perturbation Theory Calculations. *J. Chem. Phys.* **1988**, *88*, 7623–7632.

(4) Bishop, D. M.; Pipin, J.; Lam, B. Field and Field-Gradient Polarizabilities of BeH, BH and CH^+. *Chem. Phys. Lett.* **1986**, *127*, 377–380.

(5) Bishop, D. M.; Pipin, J. Field and Field-Gradient Polarizabilities of H_2O. *Theor. Chim. Acta* **1987**, *71*, 247–253.

(6) Jensen, F. *Introduction to Computational Chemistry*; 2007.

(7) Hohenberg, P.; Kohn, W. Inhomogeneous Electron Gas. *Phys. Rev.* **1964**, *136*, B864–B871.

(8) Kohn, W.; Sham, L. J. Self-Consistent Equations Including Exchange and Correlation Effects. *Phys. Rev.* **1965**, *140*, A1133–A1138.

(9) Cramer, C. J. *Essentials of Computational Chemistry : Theories and Models*; Wiley, 2004.

(10) Møller, C.; Plesset, M. S. Note on an Approximation Treatment for Many-Electron Systems. *Phys. Rev.* **1934**, *46*, 618–622.

(11) Olsen, J.; Jørgensen, P.; Helgaker, T.; Christiansen, O. Divergence in Møller–Plesset Theory: A Simple Explanation Based on a Two-State Model. *J. Chem. Phys.* **2000**, *112*, 9736.

(12) Mera, H.; Pedersen, T. G.; Nikolić, B. K. Hypergeometric Resummation of Self-Consistent Sunset Diagrams for Steady-State Electron-Boson Quantum Many-Body Systems out of Equilibrium. *Phys. Rev. B* **2016**, *94*, 165429.

(13) Frisch, M. J. et al. Gaussian 09, Revision C.02. *Gaussian 09, Revision A.02*. 2009.

(14) Hehre, W. J.; Stewart, R. F.; Pople, J. A. Self-Consistent Molecular-Orbital Methods. I. Use of Gaussian Expansions of Slater-Type Atomic Orbitals. *J. Chem.*

Phys. **1969**, *51*, 2657–2664.

(15) Collins, J. B.; von R. Schleyer, P.; Binkley, J. S.; Pople, J. A. Self-consistent Molecular Orbital Methods. XVII. Geometries and Binding Energies of Second-row Molecules. A Comparison of Three Basis Sets. *J. Chem. Phys.* **1976**, *64*, 5142–5151.

(16) Mera, H.; Pedersen, T. G.; Nikolić, B. K. Fast Summation of Divergent Series and Resurgent Transseries from Meijer- G Approximants. *Phys. Rev. D* **2018**, *97*.

Chapter 4

Conclusions and Future Work

4.1 Conclusions

The overall aim of this thesis was to take tools commonly used in computational and quantum chemistry, and help facilitate use in biological applications. In particular, we focused on the computation of nonlinear optical properties, which finds many applications in biochemistry and chemical biology. These applications include confocal microscopy, imaging for pharmaceuticals and tissues, and the development of novel biomaterials with desired optical properties.[1]

With this goal, there were two parts that needed to be investigated: (1) determining a means of computing NLO properties for common organic molecules and

polymers in a more robust manner, and (2) determine a means of computing accurate energies in a manner cheap enough to use for biological applications. The second part to this is due to the reliance of the finite field method on the computation of accurate energies.

We succeeded in making significant progress with part (1), as a variation of the finite field method that uses rational functions was studied. This investigation found that using a rational model allows for increased robustness of the method, while nearly matching the level of accuracy possible with the polynomial based finite field method. This allows for less user intervention in the method, and increased reliability, both key factors for the *in silico* screening of materials and drugs in a high-throughput fashion.

However, more work remains to be done with part (2). Though the initial results seem promising, the method must be made more reliable to be adopted and used widely. In order to do this, we must better understand why certain electron configurations and systems fail to produce accurate results consistently. Additionally, more work on finding a reliable means of optimizing the function must be conducted. However, the progress on both parts shows that it is possible to design computational tools that are relevant to biological applications, though the lens of quantum chemistry and mathematical fitting.

4.2 Future Work

Despite the work done on this topic, there are many directions that may be taken to build upon it. This includes using more general functions for nonlinear optical property prediction, to determine if the robustness can be increased further, and to determine new schemes that can be used for the purposes of resummation. Additionally, the work done in this study can be extended to other fields in quantum chemistry. For example, the idea

of using fitting functions also finds an application in the development of novel DFT methods, among many others. Finally, more user-friendly code must be written, so that the methods can be more widely (and easily) used.

Though not mentioned in the main chapters of this thesis, some preliminary work was also done using a hypergeometric function-based variant of the finite field method. Unfortunately, this work was not fruitful, as the overall optimization of the hypergeometric function consistently failed. This was likely due to the higher number of points that need to be used for the finite field method, resulting in a system of equations that was much larger and more complex than that mentioned in Chapter 3. This investigation outlines that there are limits to how complex we can make fitting functions. In future work, we will try to use different fitting functions that can be optimized linearly, or have explicit formulae to determine optimized parameters. Hopefully, this work leads to further variants of the finite field method that are increasingly robust and accurate.

Finally, we hope that the ideas presented here will be useful and applicable to other parts of quantum chemistry and not just in the scope presented here; many of the ideas adapted here originated for physics applications.

4.3 References

(1) Garmire, E. Nonlinear Optics in Daily Life. *Opt. Express* **2013**, *21*, 30532.